An Acoustic Investigation of a Coaxial Helicopter in High-Speed Flight

Gregory Walsh M.S. Candidate
Kenneth S. Brentner Professor
Department of Aerospace Engineering, The Pennsylvania State University
University Park, Pennsylvania

George Jacobellis Ph. D Candidate
Farhan Gandhi Professor
Department of Mechanical, Aerospace and Nuclear Engineering, Rensselaer Polytechnic Institute
Troy, New York

ABSTRACT

The desire for a vertical takeoff and landing (VTOL) aircraft capable of high forward flight speeds is very strong. Compound lift-offset coaxial helicopter designs have been proposed and have demonstrated the ability to fulfill this desire but, with high forward speeds, noise is an important concern that needs to be addressed. The study in this paper utilizes a Rotorcraft Comprehensive Analysis System (RCAS) model of the XH-59 aircraft, in conjunction with a noise prediction code, PSU-WOPWOP, to computationally explore the acoustics of a lift-offset coaxial helicopter. Specifically, unique characteristics of the XH-59 coaxial helicopter noise are identified; and design features and trim settings specific to a compound coaxial helicopter are considered for noise reduction. At some observer locations, there is constructive interference of the coaxial acoustic pressure pulses, such that the two signals add completely. The locations of these constructive interferences can be altered though, by modifying the upper-lower rotor blade phasing, providing an overall acoustic benefit. Significant noise reduction (and power reduction) is possible by reducing rotor tip speeds – an option available because the coaxial rotor in a compound configuration does not need to provide all the propulsive force. A dual-swept tip blade also enables noise reduction at an in-plane, forward, target observer. Compete CFD analyses, coupled with PSU-WOPWOP, should be explored in the future for a comprehensive acoustic evaluation of lift-offset coaxial helicopter noise.

INTRODUCTION

Ever since the unveiling of the first turboshaft engine powered helicopter in the early 1950's, high-speed, high-performance helicopters have been widely used in military, commercial and industrial applications. Now more commonly known as the conventional helicopter, this early vehicle concept has been redesigned and reconfigured many times in an effort to simultaneously improve performance and reduce costs. However, this helicopter today still encounters multiple problems, especially during high-speed performance, such as compressibility effects on the advancing blade, blade stall on the retreating blade, and high vehicle vibrations. In order to overcome these challenges of the conventional helicopter, alternative designs of a hover capable, VTOL aircraft have been proposed. Among these new rotorcraft configurations is the compound lift-offset coaxial helicopter.

As suggested by the name, the lift-offset coaxial rotor system has two contra-rotating rotors on the same axis, with the respective advancing sides of each rotor producing significant lift that off loads the retreating side of each rotor. This is known at the Advancing Blade Concept (ABC) (Ref. 1). In the 1970's, Sikorsky first employed the ABC rotor system on their XH-59 demonstrator helicopter in an effort to resolve the conventional helicopter's problems in high-speed forward flight mentioned earlier (Ref. 2). This coaxial rotor system is often complimented by a separate propulsive source such as a rear propeller or turbojets, as in the case of the XH-59. The compressibility effects on the advancing sides are mitigated by these auxiliary propulsion systems since the thrust requirements of the coaxial rotor systems are reduced, allowing a slower rotor rotation speed and thus, a decreased advancing-tip Mach number, M_{AT}. On the retreating side of the rotor, the blade stall is alleviated by the advancing blade's lift offset as most of the load is supported by the corresponding advancing blade on each side of the rotor disk. Furthermore, the large dynamic pressures of an advancing blade are now experienced simultaneously on each side of a lift-offset coaxial helicopter, as opposed to just on one side of a conventional helicopter rotor, which more readily enables a roll moment balance.

From the time that Sikorsky exploited these improvements of a coaxial helicopter over the conventional helicopter, those in industry, government labs and academia alike have researched high-speed, lift-offset coaxial rotorcraft. Notably, in 2009, Johnson explored how lift-offset influences the

Presented at the AHS 72nd Annual Forum, West Palm Beach, Florida, USA, May 17-19, 2016.

performance of several rotorcraft configurations, one of which was a coaxial helicopter utilizing the ABC (Ref. 3). More specific to the study here, Mosher and Peterson conducted a full-scale acoustic test of the XH-59 in the NASA Ames 40- by 80-Foot Wing Tunnel in 1983 for tunnel wind speeds between 89 and 142 kt. (Ref. 4). Recently, Jacobellis, et al. developed a model of Sikorsky's XH-59 in the Rotorcraft Comprehensive Analysis System (RCAS) to examine how control redundancies could be exploited to minimize the power requirements and hub vibrations (Ref. 5-6). The computational results from this study indicated that optimized trim settings, for a flight speed of 250 kt., reduced total power requirements by approximately 17% by reducing the main rotor RPM by 27% and decreasing the differential lateral pitch by 5 deg. For further conclusions from their study, refer to Ref. 5.

The following study aims to computationally investigate the noise characteristics of a lift-offset coaxial helicopter in high-speed forward flight, as well as identify and explain a few concerns and/or benefits of a coaxial configuration as they apply to noise. Further, this analysis explores the use of some design variables inherent to a compound lift-offset coaxial helicopter configuration, such as the XH-59, to reduce and/or control the directivity of the noise.

Review of Acoustics Theory

Prior to the noise computations, it is helpful to consider the source terms and the equation from which they come. In 1969, Ffowcs Williams and Hawkings (FW-H) derived a governing equation for noise predictions involving surfaces in arbitrary motion by creating an inhomogeneous wave equation from the Navier-Stokes equations (Ref. 7). The resulting formulation can be written as:

$$\left(\frac{1}{c_0^2}\frac{\partial^2}{\partial t^2}-\frac{\partial^2}{\partial x_i^2}\right)p'(\vec{x},t)=\frac{\partial}{\partial t}\{[\rho_0 v_n+\rho(u_n-v_n)]\delta(f)\}-\frac{\partial}{\partial x_i}\{[\Delta P_{ij}\hat{n}_j+\rho u_i(u_n-v_n)]\delta(f)\}+\frac{\partial^2}{\partial x_i x_j}[T_{ij}H(f)] \quad (1)$$

where c_0 is the speed of sound in the undisturbed medium, p' is the acoustic pressure, ρ_0 is the density of the undisturbed medium, ρ is the fluid density, v_n and u_n are the normal components of the local source surface velocity and the fluid velocity, respectively, P_{ij} is the compressive stress tensor, T_{ij} is the Lighthill stress tensor, $\delta(f)$ is the Dirac delta function and $H(f)$ is the Heaviside function. Both $\delta(f)$ and $H(f)$ use the implicit function f, which is defined as:

$$f=\begin{cases}<0 & \text{Within the data surface}\\ 0 & \text{On the data surface}\\ >0 & \text{Outside the data surface}\end{cases} \quad (2)$$

The three terms on the right hand side of the FW-H equation, Eq. (1), have mathematical characteristics of monopole (thickness noise source), dipole (loading noise source) and quadruple source terms, respectively. Thickness and loading are both discrete frequency noise sources and often large contributors to the helicopter's overall noise.

Farassat later established an integral representation of the solution to the FW-H equation, known as Formulation 1A, which neglects the quadrupole, as follows:

$$p'(\vec{x},t)=p'_T(x,t)+p'_L(x,t) \quad (3)$$

with p'_T, the thickness contribution, written as:

$$4\pi p'_T(\vec{x},t)=\int_{f=0}\left[\frac{\rho_0(\dot{v}_n+v_{\dot{n}})}{r(1-M_r)^2}\right]_{ret}dS+\int_{f=0}\left[\frac{\rho_0 v_n(r\dot{M}_r+c_0M_r-c_0M^2)}{r^2(1-M_r)^3}\right]_{ret}dS \quad (4)$$

and p'_L, the loading contribution, written as:

$$4\pi p'_L(\vec{x},t)=\frac{1}{c_0}\int_{f=0}\left[\frac{\dot{L}_r}{r(1-M_r)^2}\right]_{ret}dS+\int_{f=0}\left[\frac{L_r-L_M}{r^2(1-M_r)^2}\right]_{ret}dS+\frac{1}{c_0}\int_{f=0}\left[\frac{L_r(r\dot{M}_r+c_0M_r-c_0M^2)}{r^2(1-M_r)^3}\right]_{ret}dS \quad (5)$$

where r is the distance between the source and the observer, M_r is the Mach number in the radiation direction (from the source point to the observer), M is the Mach number of the surface $f=0$, a dot above a variable represents the source time derivative of that variable and ret denotes that each integral is evaluated at the retarded/source time. For Eq. (5) specifically, the new variable to note, *L,* is the local force per unit area, with two subscripts: *r*, to denote the radiation direction, and *M*, to indicate the forces are in a moving frame (Ref. 8).

Review of Farassat's Formulation 1A is useful because the computational acoustics software used in this study, PSU-WOPWOP, numerically solves Formulation 1A. By looking at Formulation 1A, initial expectations and concerns of coaxial helicopter noise can be drawn from this equation.

First, consider the terms on the right hand side of the thickness equation, p'_T. For a coaxial helicopter, higher forward flight speeds than a conventional helicopter are possible, resulting in larger Mach numbers around the azimuth for a given RPM. However, since the rotor rotation speed can be decreased, the Mach numbers and thus the Doppler amplification (a result of the $1/(1-M_r)$ terms) might be smaller, potentially reducing the noise and alleviating the initial high-speed noise concern.

Despite this, the presence of a second rotor still introduces additional acoustic considerations. For example, on a conventional helicopter configuration in forward flight, with an observer directly ahead of the helicopter in the rotor plane, the largest source of noise is the advancing blade because of the high Mach number and thus, a high Doppler amplification in Formulation 1A. When considering a lift-offset coaxial helicopter configuration in the same scenario, there are two blades advancing simultaneously and these large acoustic signals are constructive and add linearly. For other observer locations and situations, we expect similar linear constructive

or destructive interferences to occur between the acoustic signals from both rotors.

For the terms on the right hand side of the loading equation, p'_L, the Mach number and Doppler amplification effects are still relevant as in thickness, but, there are additional terms in the numerator to consider. Namely, the loading variables, L and $\dot{L}$, will have a very different distribution than a conventional helicopter and are likely to be impulsive in certain areas due to expected interactions such as: Blade Vortex Interactions (BVI) within each rotor, rotor-wake interactions and the various blade crossovers around azimuth. These interactions and their influence on noise will be discussed further in a later section.

SIMULATION MODEL

In order to effectively compute the noise of a lift-offset coaxial helicopter configuration, a simulation model of the XH-59 was developed in the Rotorcraft Comprehensive Analysis System (RCAS). This aircraft has two rotors, an upper counterclockwise (CCW) rotating rotor and a lower clockwise (CW) rotating rotor. Both rotors have three blades, each with a 20% root cut-out, composed of three airfoil sections: NACA 0026, 63-218, and 23012. The blade chord decreases from 20.7 inches at 20% span to 11.5 inches at the blade tips and the twist decreases from 4.6 deg. at 20% span to -3.8 deg. at the blade tips. During the rotors' rotation, the blade cross-overs occur at ψ = 0 deg. and every 60 deg. around the azimuth, where ψ denotes the rotor azimuth angle and ψ = 0 deg. points directly aft of the helicopter. The RCAS simulation uses a prescribed wake solver and the aerodynamic loads are generated at 24 spanwise locations along the quarter-chord of the blades. Output from RCAS includes blade-frame forces and moments at each of the 24 spanwise sections for both the upper rotor and the lower rotor at every degree of azimuth for one rotor rotation. Each blade on its respective rotor is assumed to experience identical loads at a given azimuth. These forces are the loading necessary to compute the loading noise contribution to Formulation 1A.

Acoustics

PSU-WOPWOP, a rotor noise prediction software utilizing Formulation 1A, is used to predict the rotor noise in this study (Refs. 9-11). From the RCAS simulation results, the aerodynamic loads are extracted and converted into PSU-WOPWOP format. A single compact loading line along the quarter-chord of each blade is generated and used in conjunction with the RCAS loads. For the thickness contribution to PSU-WOPWOP, a full distributed geometry of each blade is created with 24 spanwise nodes and 28 chordwise nodes. Each case was computed for one rotor revolution and at multiple observer locations, both in and out of the rotor plane (unless otherwise noted). For the purposes of this study, a wide variety of cases have been run and results in the following sections take the form of acoustic pressure time histories and acoustic spectra.

COAXIAL NOISE CHARACTERISTICS

The acoustic characteristics of a lift-offset coaxial helicopter are expected to be more complex than that of a single main rotor. In this section, there is an investigation into some of these complexities with a focus on specific notable characteristics of coaxial rotor noise.

Symmetry and Constructive/Destructive Interference

As a first, exploratory look into lift-offset coaxial rotor noise, a representative flight condition for the XH-59 was considered and both thickness noise and loading noise were computed. The aircraft was trimmed in RCAS with a 160 kt forward flight speed, at 335 RPM, and an angle of attack of 4 deg., yielding an M_{AT} = 0.8.

In Fig. 1, the in-plane thickness acoustic pressure time history and thickness spectra for one rotor revolution at five in-plane observer locations, equally spaced around the forward azimuth from ψ = 90 deg. to ψ = 270 deg., each at a distance of 10 rotor radii from the hub (Note: azimuth angles referenced in this study are relative to the upper, CCW rotor). For this plot and the subsequent in-plane plots in this paper, computations for eight in-plane observers, equally spaced around the entire azimuth, were preformed, but only these five in-plane observers have relatively strong acoustic signals in high-speed forward flight; therefore, only these five are reported.

The thickness noise generated by each of the rotors is symmetric with respect to the centerline of the rotorcraft (assuming they have the same geometry, mirrored as appropriate for rotation in the opposite direction), as shown in Fig. 1. This is true because the thickness noise is only a function of the blade geometry and operating conditions – not the blade loading. The impact of this symmetry is that the thickness noise is doubled on the plane of symmetry, also seen in Fig. 1. This is a property that will generally be applicable to the loading noise as well; however, the loading on the two rotors will not be identical, resulting in loading noise that is not symmetrical.

At locations off the plane of symmetry, the distance from the sources to the observer are different; hence, there is a time delay and a decay for the more distant source (most noise comes from the blade tip region on the advancing sides of the rotors). This results in constructive and destructive interference between the rotors. This can be clearly seen in Fig. 1 for observer locations that are not on the plane of symmetry (i.e., not $\psi = 180$ deg.). For example, at $\psi = 135$ deg., there are three thickness noise pulses that are larger than the other three (spherical spreading), and the smaller pulses are not centered between the larger pulses (time delay). It is clear in Fig. 1 that at $\psi = 180$ deg. there is constructive interference – the two signals add completely. At other locations, a positive part of the acoustic pressure time history can add with the negative part of the other rotor signal; hence,

destructive interference. The same effect is true for all rotor noise sources, although thickness noise is very symmetric.

Loading: Blade Crossovers & BVI

Though the previous section focused primarily on thickness noise, the loading noise from a lift-offset coaxial rotor has unique properties as well. Fig. 2 shows the lift distribution (in lb) on both the upper and lower rotors, respectively. On the advancing side of each rotor, the loading experiences multiple instances of impulsive loading changes, likely caused by BVI within each rotor, rotor-wake interactions between the two rotors or the aerodynamic interference when the rotors "cross". In addition, Fig. 2 highlights the feature of a lift-offset coaxial rotor that the majority of the lift is produced on the advancing side of the rotor disk, and in this case, by the inboard sections of the blades, rather than the blade tips.

From an acoustic perspective, there are at least two interesting features in the blade loading shown in Fig. 2. First, the rapid or impulsive loading changes are very important, likely to cause significantly strong and impulsive loading noise pulses. Secondly, moving the loading inboard and away from the tip, causes the Doppler amplification to have a less predominant role (although this is generally not as important for loading noise).

Since loading noise is dominant for observer locations out of rotor plane observer, only those will be reported here; and Figs. 3 and 4 display the loading acoustic pressure time histories and loading spectra at four azimuth angles (0 deg., 90 deg., 180 deg. and 270 deg.) and three elevation angles below the rotor (-15 deg., -45 deg. and -75 deg.), each at a distance of 10 rotor radii from the hub.

Reviewing Figs. 3 and 4, impulsive BVI noise-like pulses are evident in the loading noise, but they are larger for observer locations farther from the rotor tip-path plane. Excitation such as these are not always present, nor as strong, with a single main rotor aircraft but the addition of a second rotor results in interactional loading not experienced by a single rotor.

Coaxial vs. Conventional – Thickness Noise

As a further examination of lift-offset coaxial helicopter noise characteristics, thickness noise results for the XH-59 are compared to results of a solidity equivalent, notional, single main rotor conventional helicopter in the same flight condition as previously described. This notional single main rotor model was created from the XH-59 coaxial model by taking the three blades on the lower rotor and adding them to the upper rotor, generating a 6-bladed single main rotor, rotating CCW. Although this single main rotor helicopter configuration is not optimally designed and may not be realistically flown, it provides a useful acoustic comparison to reveal important differences between single main rotor and coaxial rotor noise.

Fig. 5 presents the thickness noise component in the same format as Fig. 1 but with the additional single rotor results for comparison. As illustrated in Fig. 5, thickness noise for the coaxial configuration is larger, or at least similar to, the conventional single main rotor configuration at all in-plane observers. Furthermore, the constructive interference of the coaxial thickness noise at $\psi = 180$ deg. is strikingly clear; with acoustic pressure pulses of double the strength and twice the amount of spectra frequency content than the single rotor configuration.

BLADE CROSSOVER COMPARISON

A few unique properties and characteristics of coaxial rotor noise have been presented and pose some concerns of high noise levels for certain observer locations, namely thickness noise in the rotor plane at ψ = 180 deg. and loading/BVI noise below the rotor plane. An interesting area to explore, with this knowledge, is the impact different lift-offset coaxial helicopter design variables and/or trim settings (available due to control redundancies) can have on the noise, specifically focused on noise reduction.

The first design parameter considered is the relative blade phasing or blade clocking, effectively altering the azimuth angles at which the upper rotor blades and the lower rotor blades cross. Theoretically, changing this variable will alter the locations of constructive and destructive interference and shift the impulsive loading locations experienced on the advancing sides of each rotor for potential BVI/loading noise mitigation.

As a baseline case, the originally designed blade crossovers of ψ = 0 deg. and every 60 deg. after that around the azimuth will be used. Initial crossover locations of ψ = 0 deg. through ψ = 60 deg. (baseline case again) in increments of 10 deg. are considered. The best and most interesting results occur when the blades cross at ψ = 30 deg. and every 60 deg. after that around the azimuth. A comparison of the noise for this phasing configuration to the baseline case are presented and discussed below. In both cases, the XH-59 RCAS model is trimmed with a forward flight speed of 230 kt., at an RPM of 179, resulting in a 0.64 M_{AT}, with an angle of attack of 3 deg.

Total Noise

As a preliminary result, Figs. 6, 7, and 8 show the total noise comparison of both blade crossover positions for in-plane and out-of-plane (below plane) observers, respectively. In Fig. 6, the total in-plane noise shows no clear indication that either blade crossover configuration provides a substantial acoustic benefit relative to the other, as each signal is stronger at one observer location and then weaker at another; but it is clear that both cases have significant impulsive content.

The out-of-plane observers, Figs. 7 and 8, however, tell a different story. While it is true that both signals continue to be impulsive in nature, changing the initial crossover location to ψ = 30 deg., from the original ψ = 0 deg. design, is quieter at most observer locations below the rotor plane. Furthermore, directly below the rotors, the sound pressure level (SPL) is higher by 5 to 10 dB at nearly all frequencies for the baseline case. For a deeper understanding and a better comparison, it is useful to separately consider the thickness and loading components.

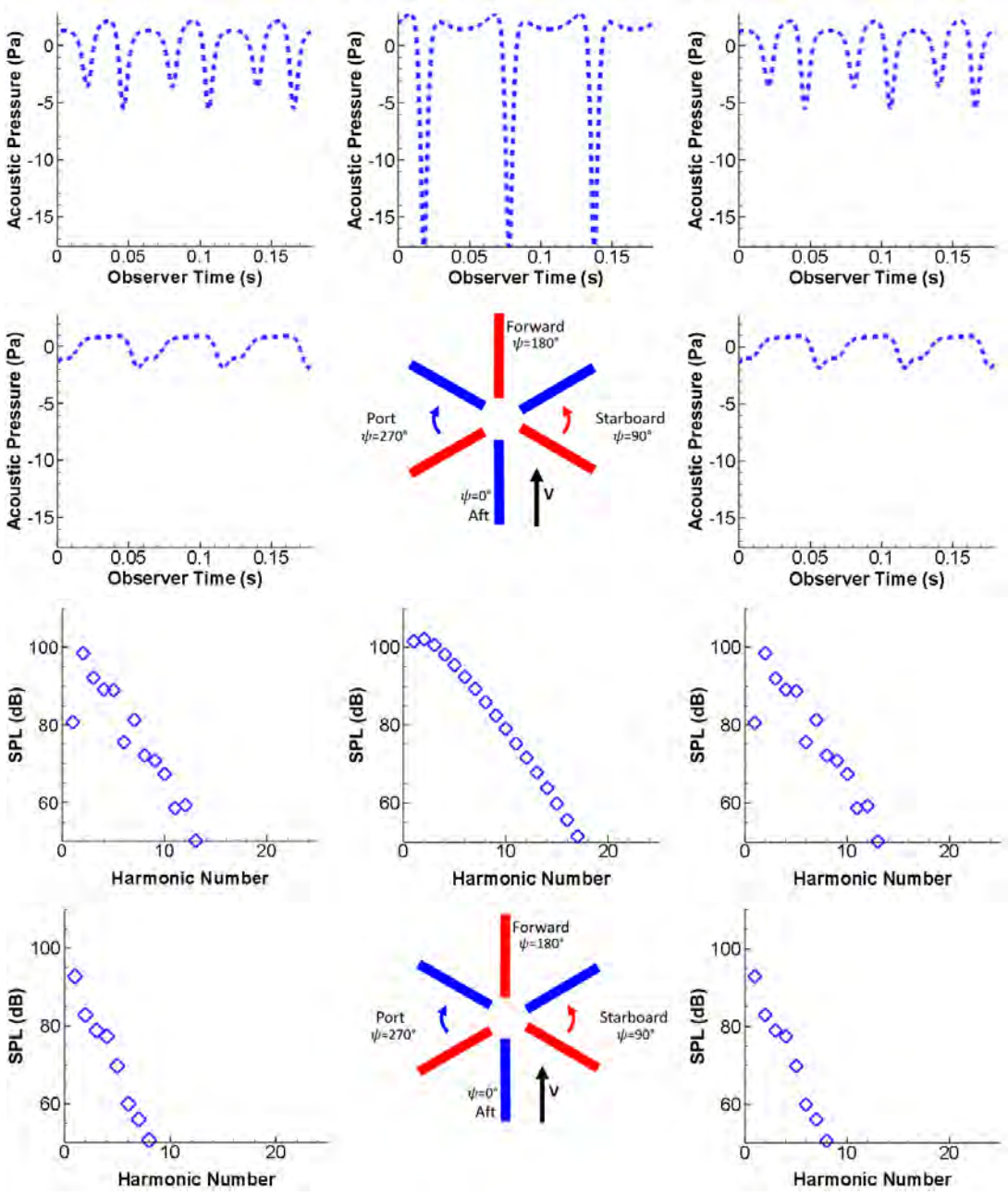

Figure 1. Thickness noise at in-plane observers of the coaxial rotor (·····◇ Coaxial).

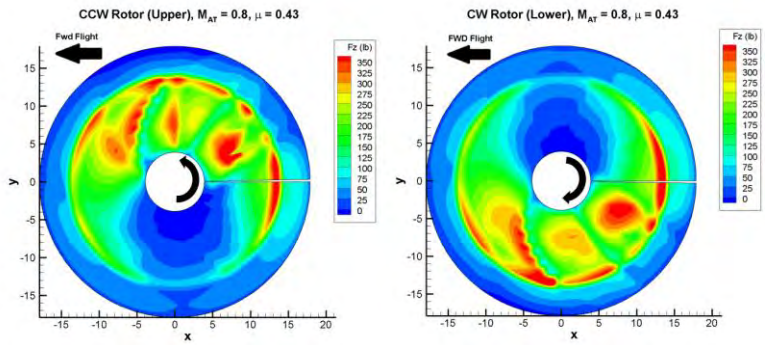

Figure 2. Upper and lower rotor lift distribution on rotor disk plots for 160 kt. forward flight speed at 335 RPM.

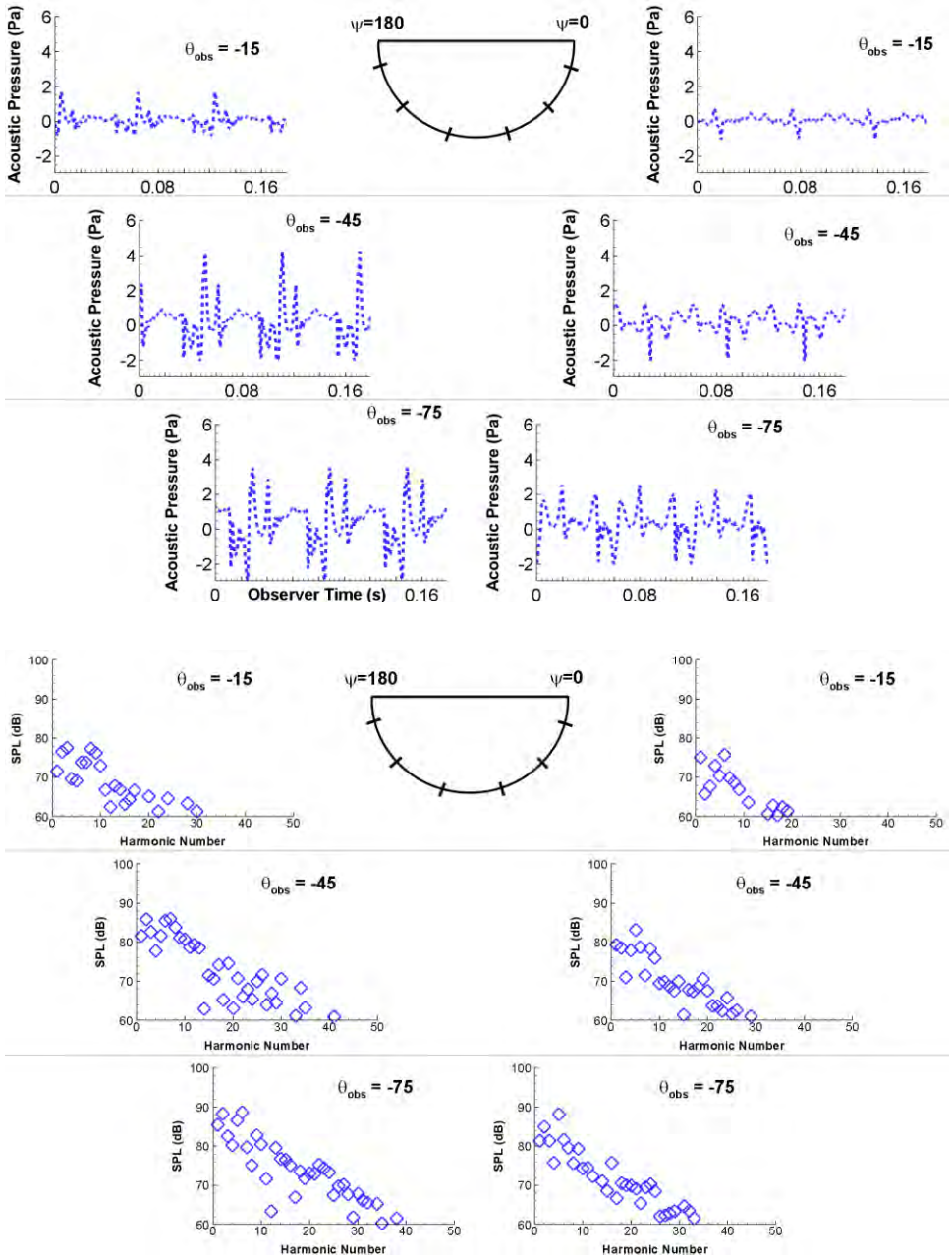

Figure 3. Loading noise at out-of-plane ψ = 0 and 180 deg. observers of the coaxial rotor (◇ Coaxial).

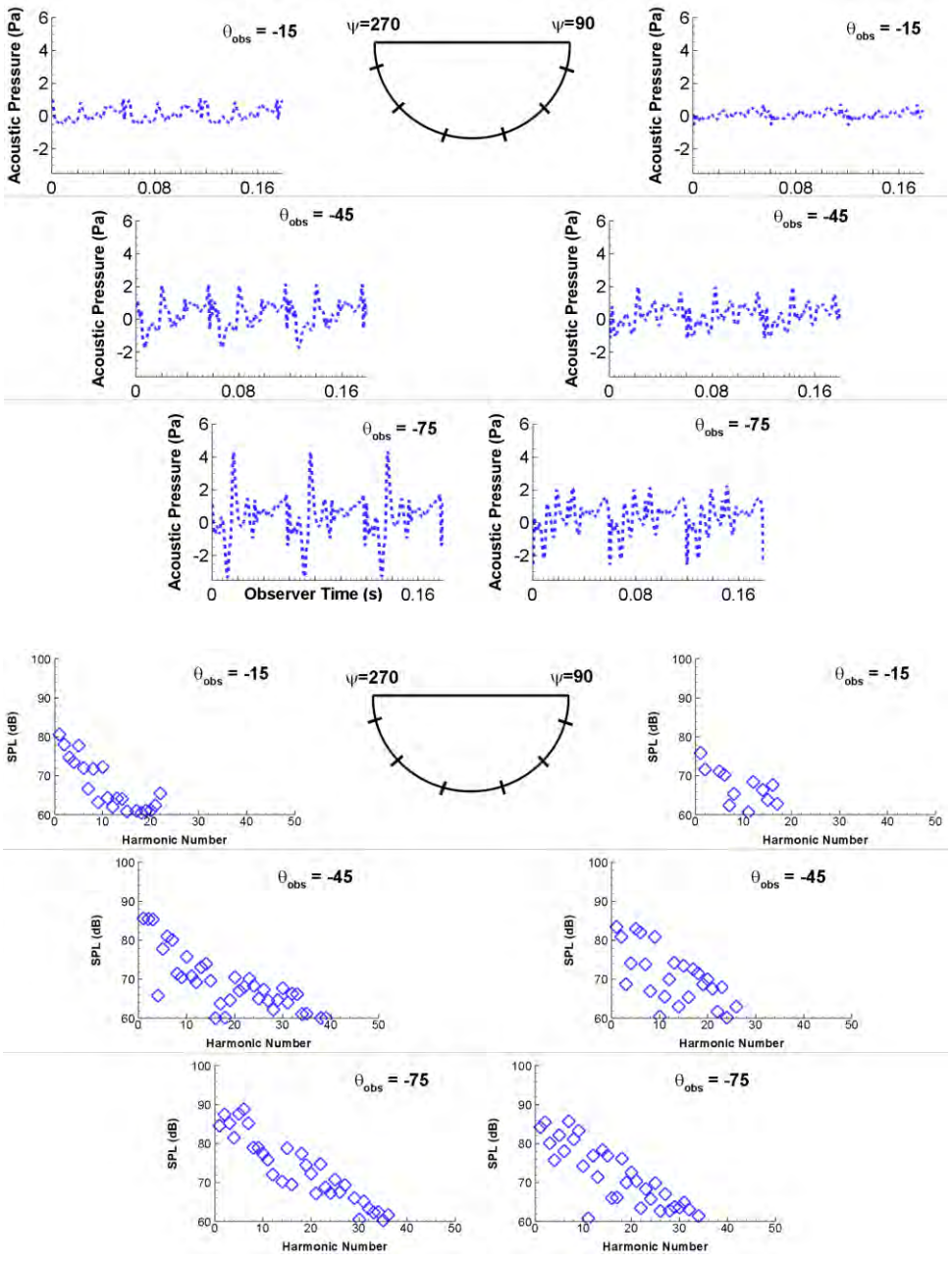

Figure 4. Loading noise at out-of-plane ψ = 90 and 270 deg. observers of the coaxial rotor (◇ Coaxial).

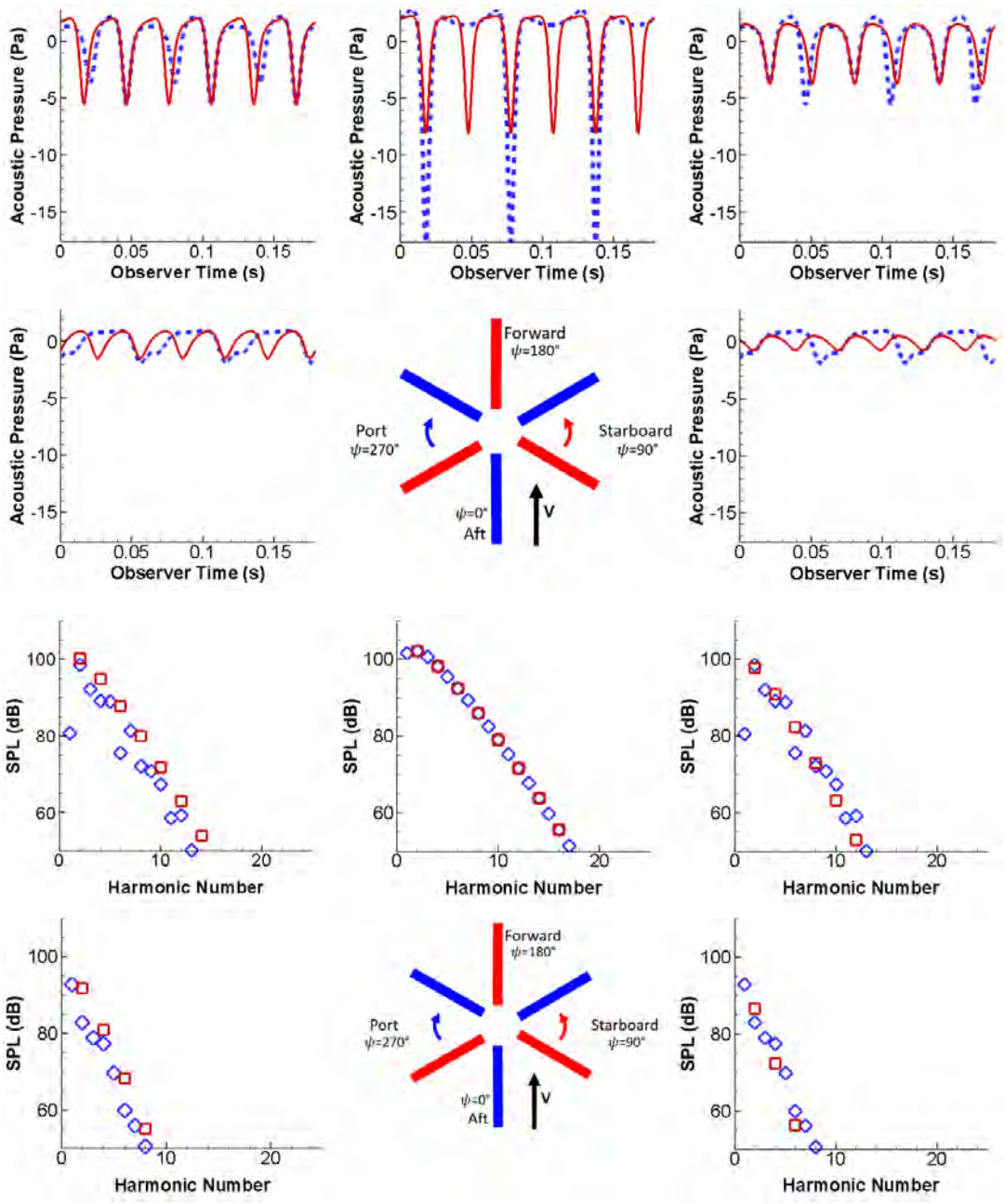

Figure 5. Comparison of thickness noise at in-plane observers of single rotor vs. coaxial rotor.
(□ Single, ◇ Coaxial).

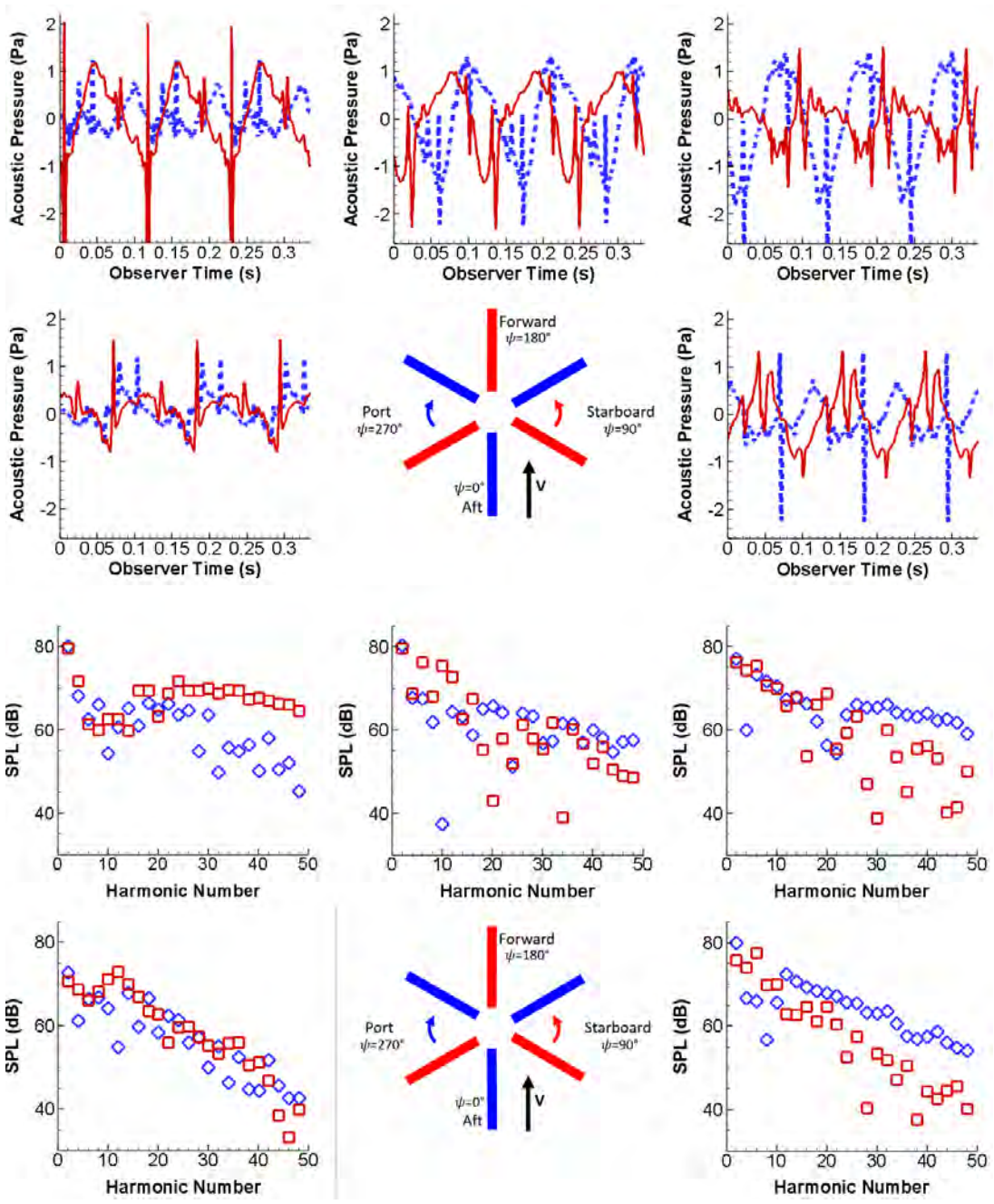

Figure 6. Comparison of total noise at in-plane observers for ψ = 0 deg. crossover vs. ψ = 30 deg. crossover.
(——— □ ψ = 0 deg. crossover, ------- ◇ ψ = 30 deg. crossover).

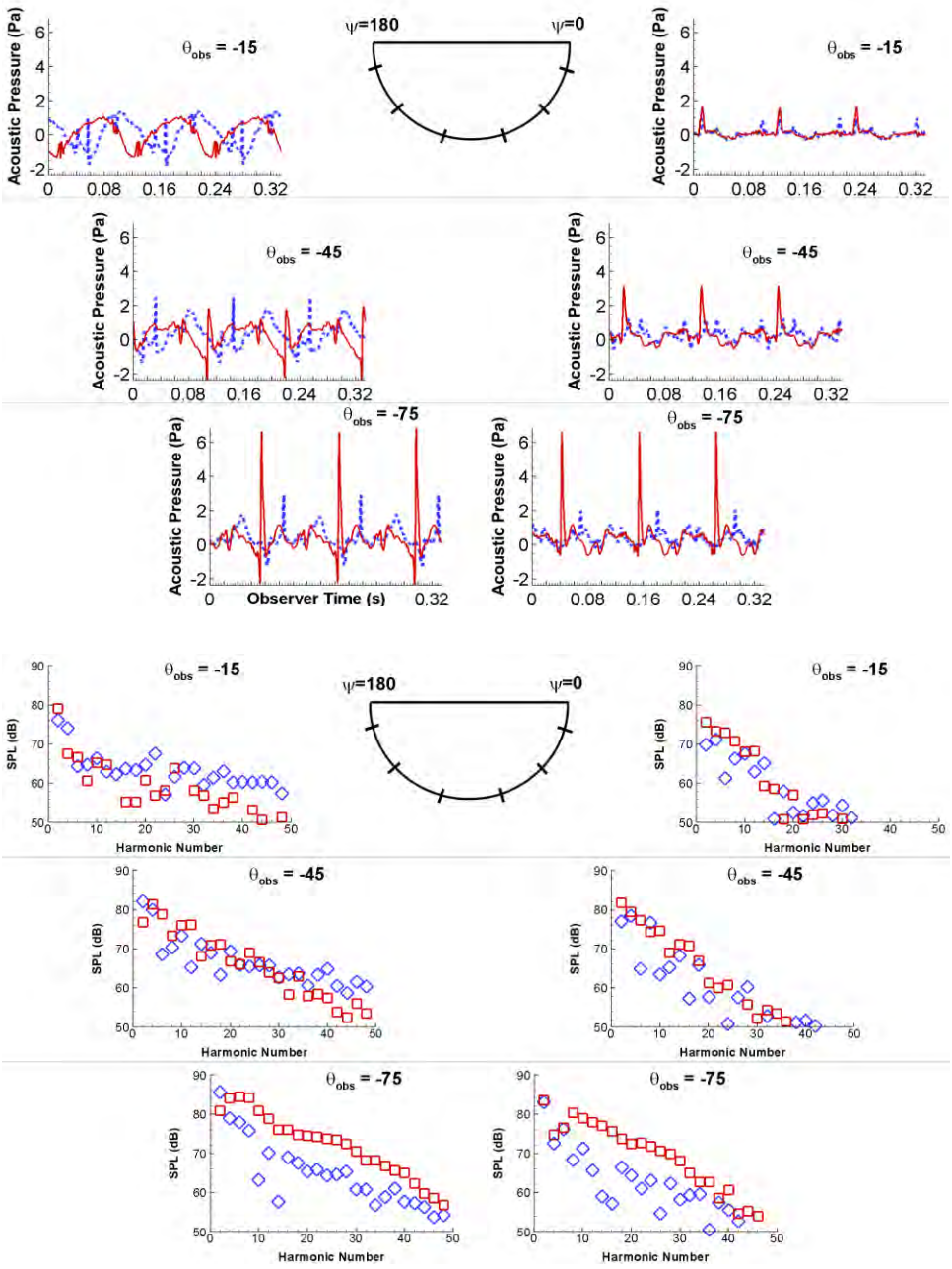

Figure 7. Comparison of total noise at out-of-plane ψ = 0 and 180 deg. observers for ψ = 0 deg. crossover vs. ψ = 30 deg. crossover (□ ψ = 0 deg. crossover, ◇ ψ = 30 deg. crossover).

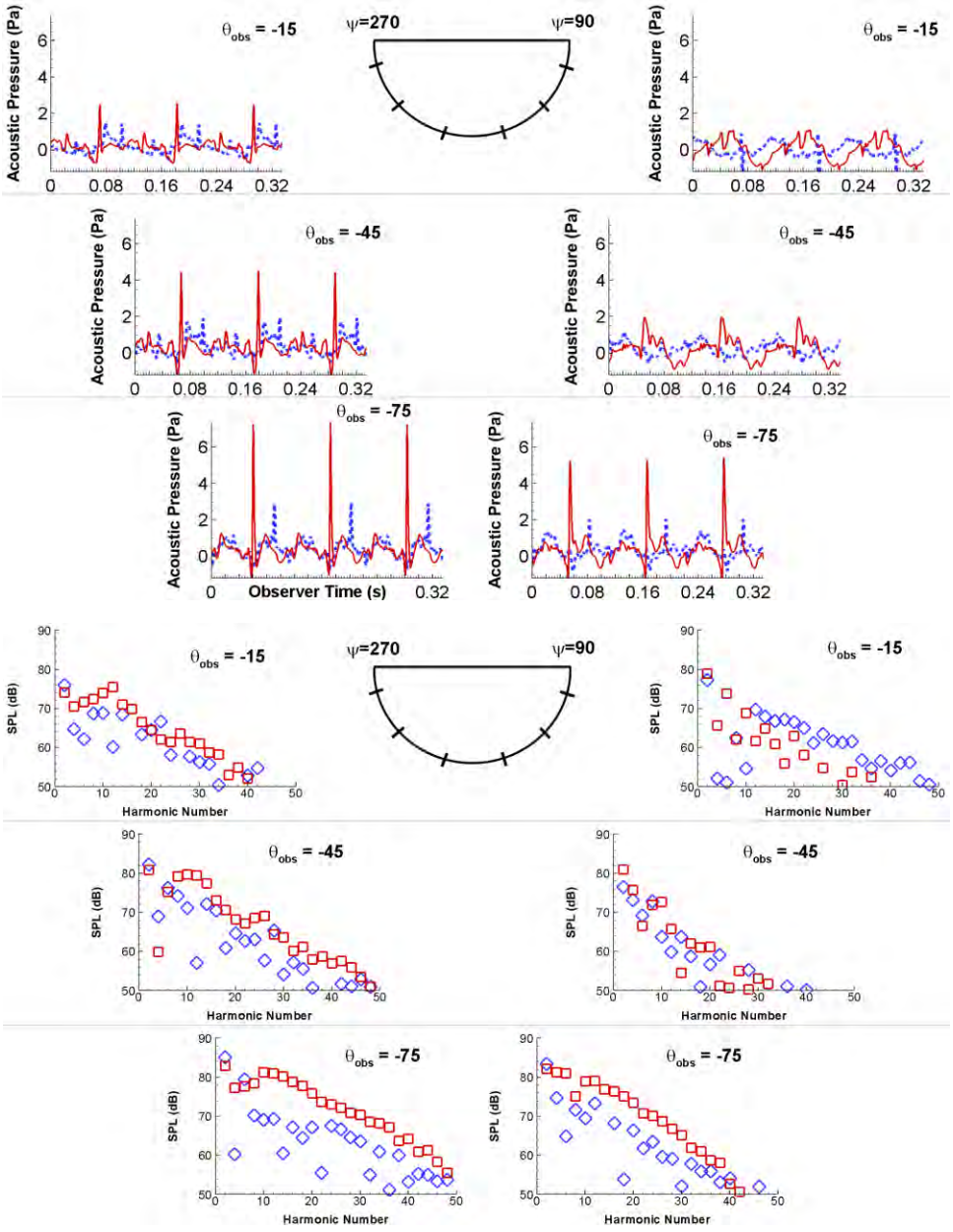

Figure 8. Comparison of total noise at out-of-plane ψ = 90 and 270 deg. observers for ψ = 0 deg. crossover vs. ψ = 30 deg. crossover (□ ψ = 0 deg. crossover, ◇ ψ = 30 deg. crossover).

Thickness

Figures 9, 10 and 11 display thickness noise plots for in-plane and out-of-plane observers respectively, in the same manner as before. As illustrated in Fig. 9, there is a clear benefit at the forward in-plane observer location to changing the blade phasing from the baseline case. These large thickness acoustic signals at ψ = 180 deg. no longer have constructive interference with one another when the initial blade crossover position is changed to ψ = 30 deg. and this observer is no longer the dominant observer location of in-plane noise. Instead, the constructive inference and largest in-plane thickness acoustic pulses are located at the ψ = 135 and 225 deg. locations (as well as at ψ = 45 and 315 deg. locations, though not as significant). This case is representative of how in-plane thickness noise for a lift-offset coaxial rotor can potentially be optimized for desired noise abatement at target observer locations by utilizing blade phasing. Furthermore, for a case with a higher RPM and thus, higher M_{AT}, this blade crossover change will be even more acoustically advantageous as the forward, ψ = 180 deg. observer signal strength substantially increases with M_{AT} and becomes significantly more dominant compared to other in-plane observers.

Moreover, it is important to point out that the in-plane thickness spectra plots are largely affected by this blade crossover change. The spectral points of the two crossover cases match at every other harmonic and the original blade crossover, ψ = 0 deg., has twice the amount of points.

The out-of-plane comparison of thickness noise for these two blade crossover cases, shown in Figs. 10 and 11, is less interesting than the in-plane results. Only at the ψ = 180 deg. observer is the change in blade crossover position noticeably beneficial, which we previously established by looking at the in-plane thickness noise. This is not surprising, however, since typically thickness noise is dominant in-plane and loading dominant out-of-plane. Thickness noise also typically has low frequency content, as is the case here.

Loading

In the same manner as thickness noise, the loading noise is compared for the blade crossover cases with in-plane and out-of-plane results shown in Figs. 12, 13 and 14, respectively. Comparing the in-plane loading noise to the in-plane thickness noise reveals that the loading is the larger noise component in the rotor plane – which is not normally the case. Therefore, the conclusions are the same as for total noise. The in-plane loading noise shows no uniform acoustic benefit due to altering the blade crossover location but instead, can enable some directivity control.

Contrary to the in-plane results, the out-of-plane loading noise comparison of blade crossover locations provides very interesting outcomes. In both out-of-plane plots, Figs. 13 and 14, the overall strength of the loading acoustic pulses is reduced at nearly all observer locations by changing the blade crossover positions from the baseline to the ψ = 30 deg. crossover configuration. Most significantly, the strongest loading acoustic pulses in both out-of-plane plots, at $\theta_{obs} = -75$ deg. elevation, are reduced to a third of the original signal. This is evident in both the time-history and spectral plots.

By digging deeper and considering the rotor loading for each crossover configuration, shown in Figs. 15 and 16 for the upper, CCW rotors and lower, CW rotors respectively, some insight can be gained as to why the new crossover configuration provides an acoustic benefit. In both Figs. 15 and 16, the black dash-dot lines represent the locations of blade crossovers for each rotor configuration and ψ = 180 deg. is located at the left most point of the circle at y= 0. As illustrated by Fig. 15, comparing both upper, CCW rotors, there is not a large noticeable difference between the two contour plots; each appears to have an impulsive loading change around ψ = 70 deg. and the baseline configuration does have a second instance of that around ψ = 120 deg., though it doesn't seem to be very significant. The rotor disk loading in Fig. 16, of the lower, CW rotors, however, are distinctly different in a few ways (Note: for this brief section, the rotor azimuth angles are in the CW convention, such that the advancing blade at ψ = 90 deg. points directly down at $x = 0$ on the rotor disk plots). First, the inboard region of high lift begins at a different azimuth for each configuration; around ψ = 60 deg. for the baseline case and around ψ = 30 deg. for the new configuration. It is also interesting to note that in both cases, these regions begin at, or shortly after, a blade crossover with the upper rotor. Furthermore, there is an impulsive loading change on the advancing blade of the baseline case, directly at a blade crossover location of ψ = 120 deg., which is not present in the new configuration.

These different characteristics result in significant reduction in the impulsiveness of the loading noise by altering the upper to lower rotor blade phasing, which suggests that the large acoustic pulses shown in Figs. 13 and 14 could be excited by the specific baseline configuration and mitigated by altering the blade crossover locations. Moreover, while it was originally thought that either blade crossovers or BVI events (self-generated BVI) caused the impulsive loading noise below the rotor plane, the impact of changing the blade crossover positions has on this noise indicates that perhaps it is more likely the blade crossovers or even BVI from the upper rotor into the lower rotor that is causing this noise. A further study would be valuable to more completely understand the cause of the impulsive loading and noise.

Although the acoustic benefit was not conclusive by only considering the in-plane loading noise, the out-of-plane loading noise results display a strong advantage to modifying the original blade crossover configuration into a new blade phasing where blades of the upper and lower rotor crossover at ψ = 30 deg. and every successive 60 deg. around the azimuth.

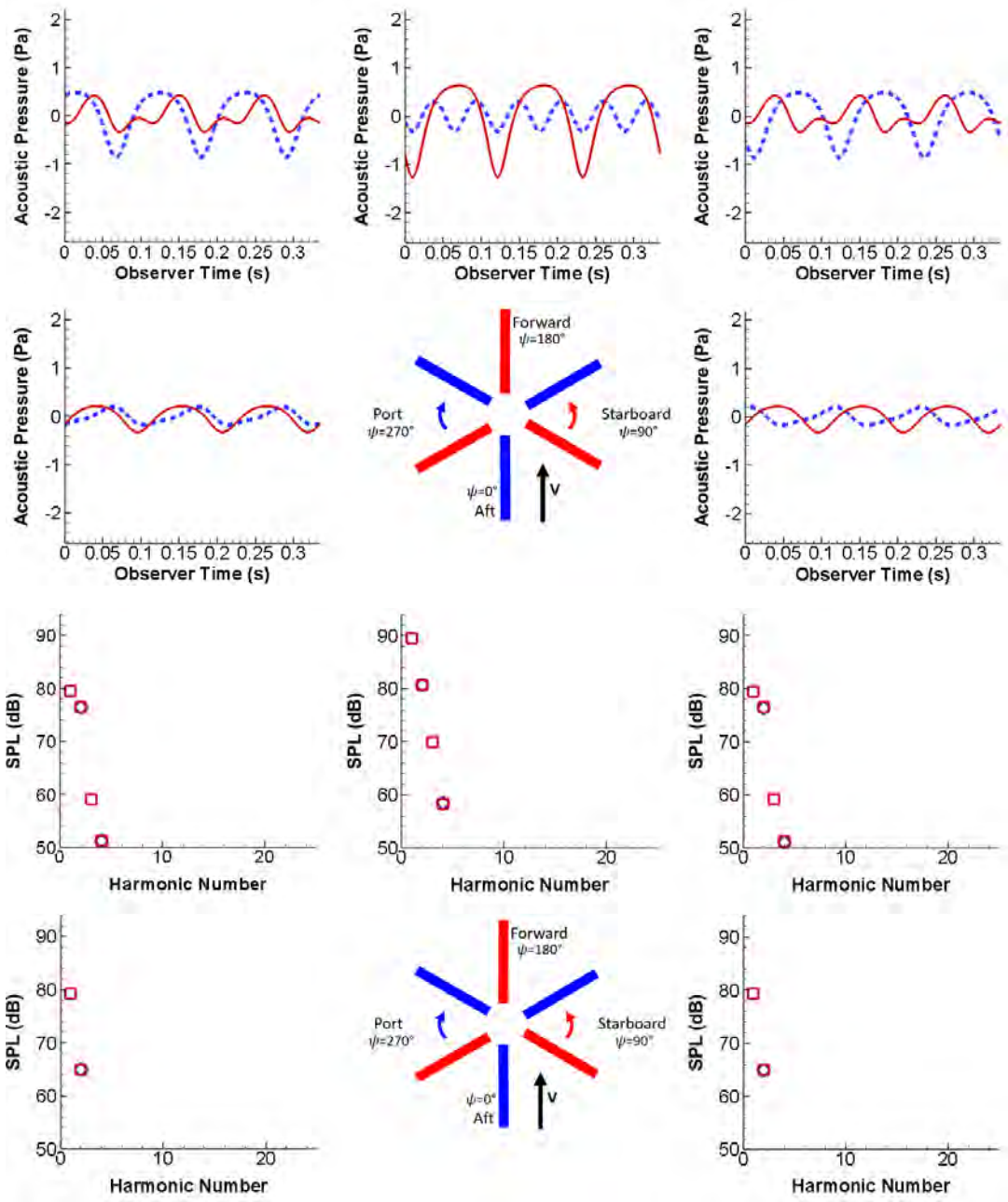

Figure 9. Comparison of thickness noise at in-plane observers for ψ = 0 deg. crossover vs. ψ = 30 deg. crossover. (—□— ψ = 0 deg. crossover, ·····◇····· ψ = 30 deg. crossover).

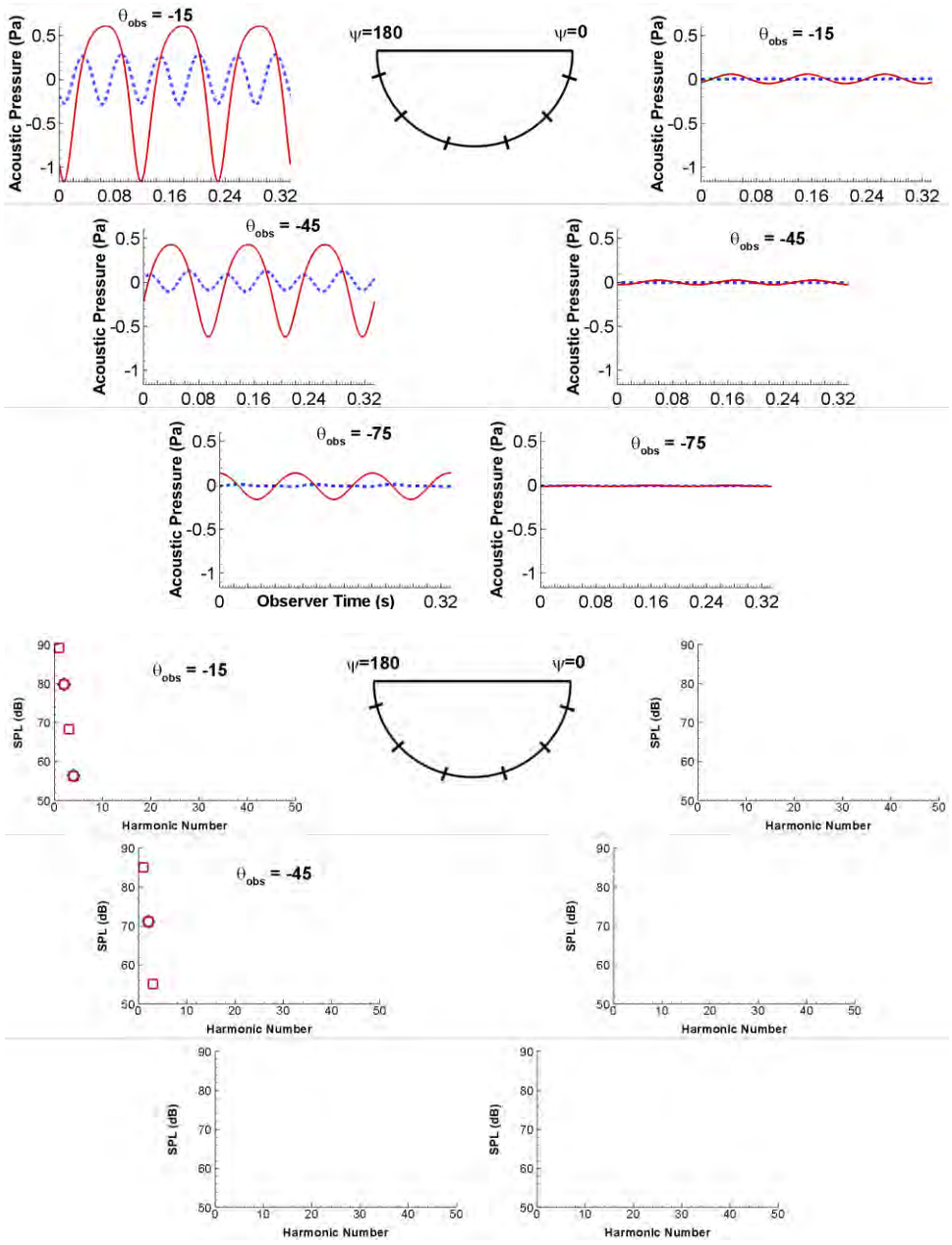

Figure 10. Comparison of thickness noise at out-of-plane ψ = 0 and 180 deg. observers for ψ = 0 deg. crossover vs. ψ = 30 deg. crossover. (—— □ ψ = 0 deg. crossover, ····· ◇ ψ = 30 deg. crossover).

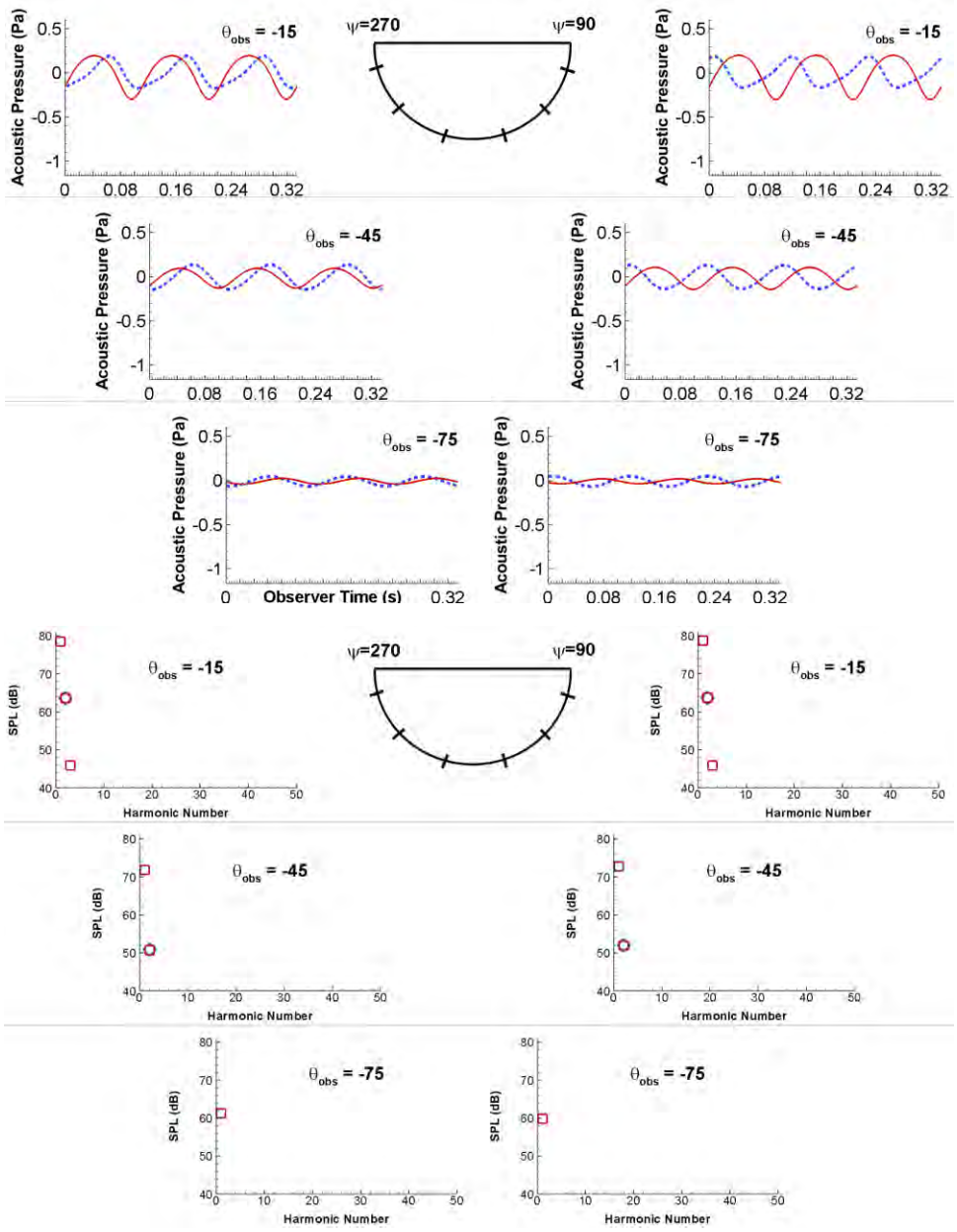

Figure 11. Comparison of thickness noise at out-of-plane ψ = 90 and 270 deg. observers for ψ = 0 deg. crossover vs. ψ = 30 deg. crossover. (□ ψ = 0 deg. crossover, ◇ ψ = 30 deg. crossover).

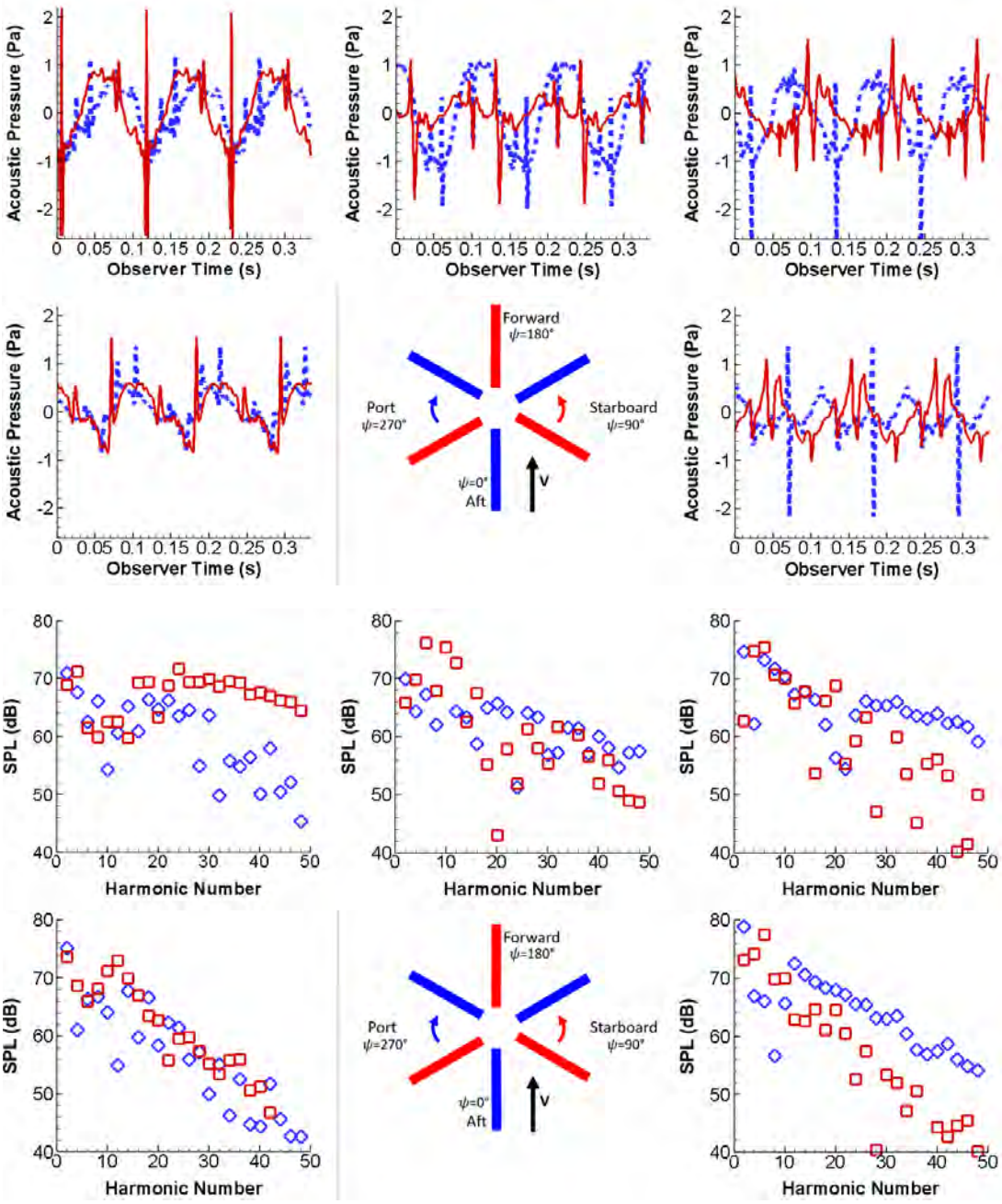

Figure 12. Comparison of loading noise at in-plane observers for $\psi = 0$ deg. crossover vs. $\psi = 30$ deg. crossover. (——— □ $\psi = 0$ deg. crossover, ------- ◇ $\psi = 30$ deg. crossover).

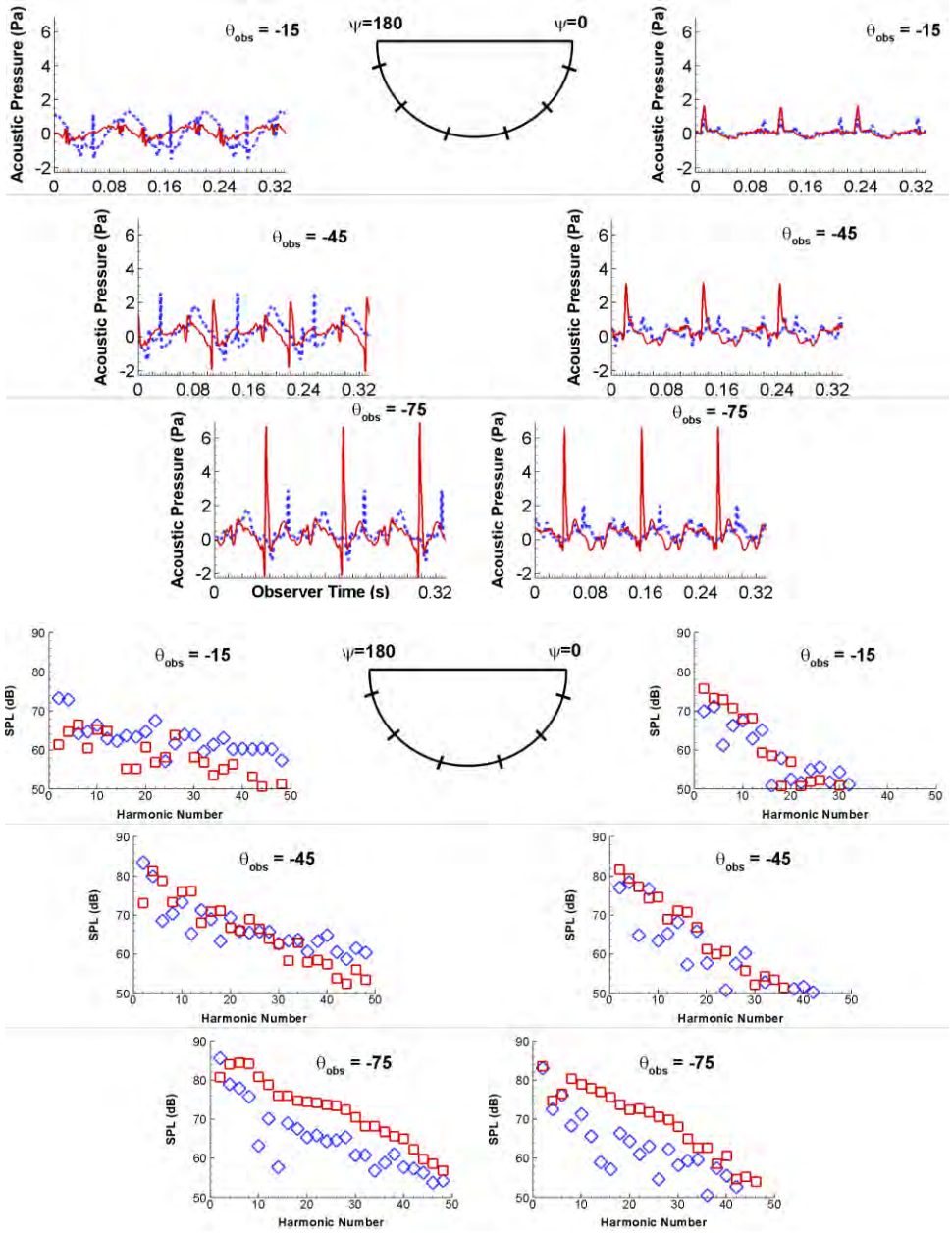

Figure 13. Comparison of loading noise at out-of-plane $\psi = 0$ and 180 deg. observers for $\psi = 0$ deg. crossover vs. $\psi = 30$ deg. crossover. (□ $\psi = 0$ deg. crossover, ◇ $\psi = 30$ deg. crossover).

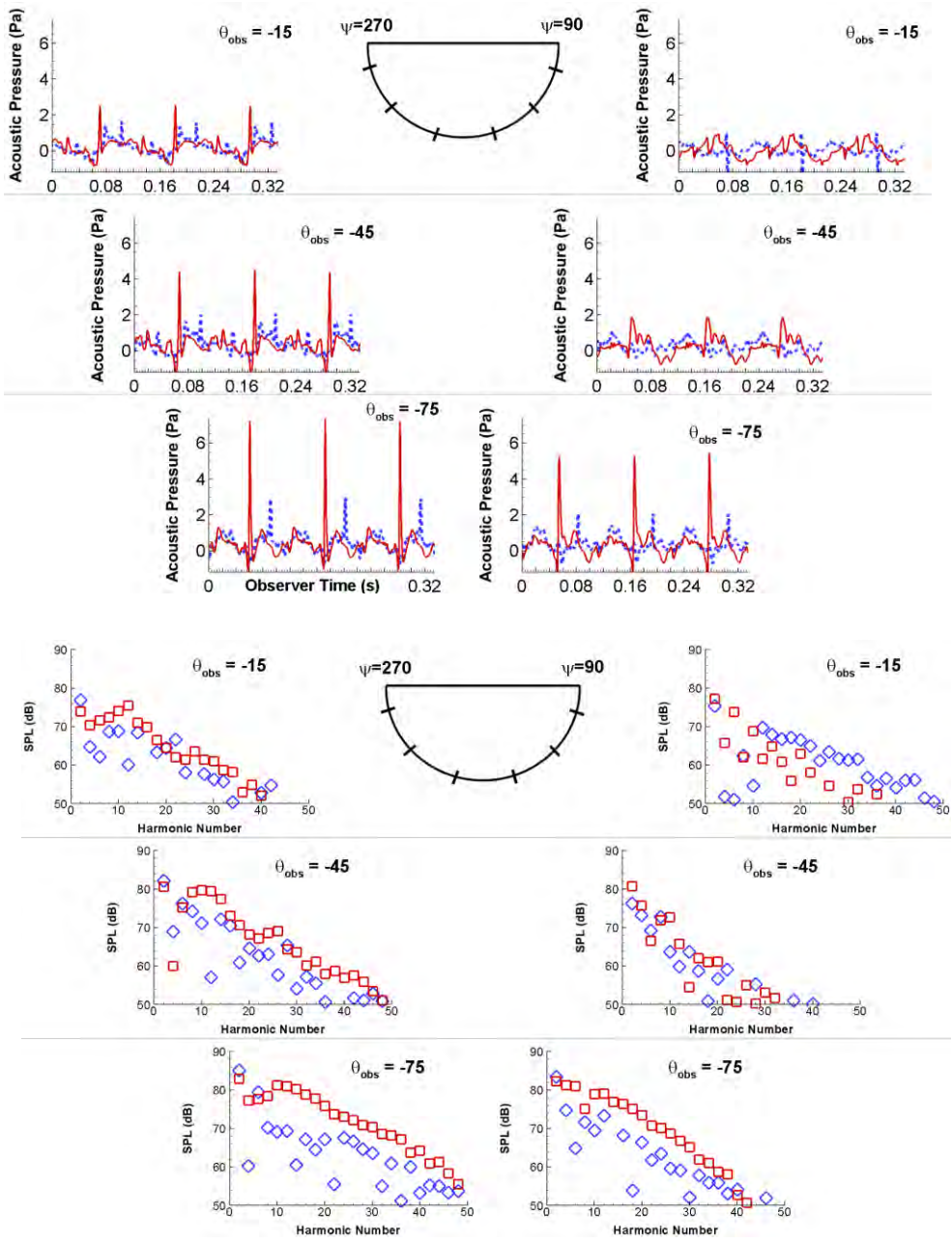

Figure 14. Comparison of loading noise at out-of-plane ψ = 90 and 270 deg. observers for ψ = 0 deg. crossover vs. ψ = 30 deg. crossover. (□ ψ = 0 deg. crossover, ◇ ψ = 30 deg. crossover).

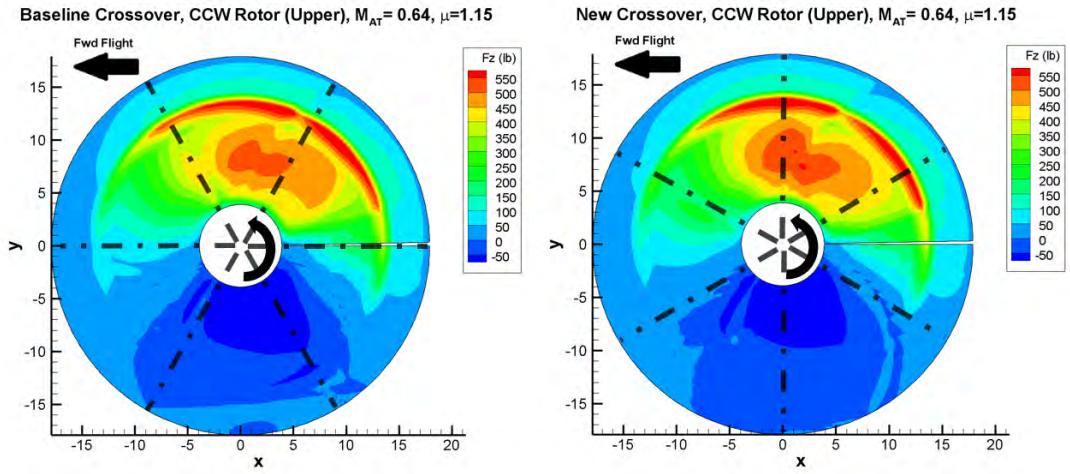

Figure 15. Comparison of CCW, upper rotor lift distribution on rotor disk plots for ψ = 0 deg. crossover (left) vs. ψ = 30 deg. crossover (right). Black dash-dot lines represent blade crossover locations.

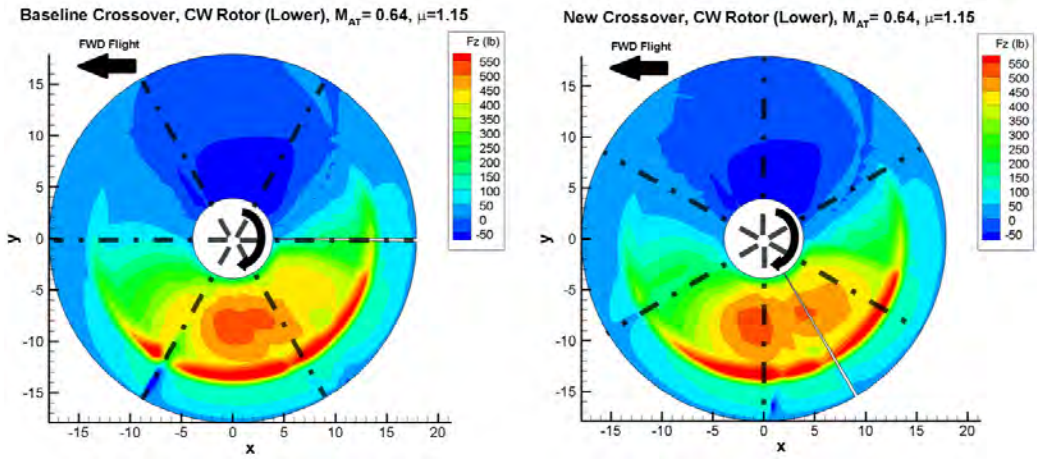

Figure 16. Comparison of CW, lower rotor lift distribution on rotor disk plots for ψ = 0 deg. crossover (left) vs. ψ = 30 deg. crossover (right). Black dash-dot lines represent blade crossover locations.

RPM REDUCTION STUDY

The blade crossover locations of the upper and lower rotor proved to be an important acoustic factor, primarily for the out-of-plane loading noise. A second lift-offset coaxial helicopter parameter, the rotors' RPM, is also acoustically considered (Note: the XH-59 is a compound helicopter and rotor RPM is a trim variable).

As previously seen in Farassat's Formulation 1A, the powers of the Doppler amplification in the each of the acoustic pressure terms, have a strong influence on the noise and because M_r varies linearly with RPM for a fixed flight speed, varying the RPM is expected to have a significant impact on the overall noise.

Though the XH-59 has a maximum design RPM of 345, for the purposes of this study and for realistic forward flight trim, settings for a slowed rotor were compared: RPMs of 179, 207 and 276 (52%, 60% and 80% of maximum RPM respectively). In each case, the helicopter was trimmed with a forward flight speed of 230 kts, resulting in M_{AT} = 0.64, 0.69, and 0.81 for 179, 207 and 276 RPM respectively, and an angle of attack of 3 deg. for all three cases. Additionally, although the upper to lower rotor blade phasing was shown to be effective in noise reduction, the blade phasing in this comparison was kept as originally designed on the XH-59.

Total Noise

In the same manner as the blade crossover study, Figs. 17, 18 and 19 show the total noise first for both in-plane and out-of-plane observers, respectively. It should be noted that the *x*-

axis in all the plots in this RPM reduction study are "Fraction of Revolution" ranging from 0 to 1 or "Harmonic Number", which both normalize the rotor rotation speed for easier comparisons between RPMs. Upon looking at the total in-plane results in Fig. 17, it is immediately clear that reducing the rotor RPM has a significant impact on reducing the overall in-plane noise and most effectively at the forward, $\psi = 180$ deg. observer, where the in-plane noise is dominant.

Likewise, the out-of-plane plots in Figs. 18 and 19 show a noise reduction with RPM reduction; but, at some out-of-plane observers, the opposite is true: the noise increases with an RPM decrease, which is an area that needs to be further examined by separately considering thickness and loading noise.

Thickness

Thickness noise is largely dominant within the rotor plane and often not out of the rotor plane, thus, Fig. 20, shows an in-plane thickness noise comparison of the three rotor RPM cases and the corresponding out-of-plane results will not be discussed, though they were computed. As displayed by these plots, the reduction in rotor RPM results in a dramatic reduction in thickness noise at all in-plane observers. This decrease is so substantial that the acoustic pulses of the 179 RPM case can hardly be seen when plotted on the same scale as the 276 RPM case. However, the thickness noise reduction is not a huge surprise when considering the Doppler factor in Farassat's Formulation 1A. As mentioned before, the Doppler amplification and the Mach number of the blades have a large influence on the thickness noise and this impact is twofold when considering the presence of constructive interference at some in-plane observers. By making a large reduction in the RPM, the Mach number on the blades is proportionally reduced, despite maintaining the helicopter's forward flight speed, which leads to this large reduction in the thickness noise signal. Clearly, a reduction in rotor RPM is perhaps the most effective parameter for reducing the in-plane thickness noise and the overall noise signature of a lift-offset coaxial helicopter, such as the XH-59.

For further reference and to understand the magnitude of the impact of this rotor RPM reduction, an additional case was run with the XH-59's design RPM of 345 and the in-plane thickness noise is compared to the 276 and 179 RPM cases and shown in Fig. 21. Though high-speed impulsive (HSI) noise is not accounted for and would likely more than double the acoustic pressure pulse for the 345 RPM case, it is still evident that flying with a slowed rotor RPM, is perhaps the most effective approach to mitigate the noise. Moreover, for a first principles, in-plane thickness noise abatement procedure of a compound lift-offset coaxial helicopter, the RPM should be highly considered since high forward flight speeds can be maintained.

Loading

Since it has been established that thickness noise is greatly reduced with RPM, loading noise is now considered and shown for both in-plane and out-of-plane observers in Figs. 22, 23 and 24. For the five in-plane observers in Fig. 22, it is interesting to note that the RPM appears to have the opposite effect on loading noise as it did on thickness noise. The loading noise at in-plane observers actually increases with a decrease in RPM. Despite this increase, when the in-plane loading noise is considered on the scale of the in-plane thickness noise, this increase is not very significant.

In Figs. 23 and 24, a similar phenomenon is seen for loading noise at out-of-plane observers. The loading noise is similar between the RPMs for most out-of-plane observers but observers at an elevation angle of -75 deg. experience an increase in the loading noise signal with a decrease in RPM. Specifically, large, narrow acoustic pulses become present as the RPM is decreased to 179. By comparing the rotor loading plots for these RPM cases, shown in Figs. 25, 26 and 27 for 276, 207 and 179 RPM respectively, an increase can be seen in the amount of high lift regions and the number of impulsive loading areas along the advancing sides as the RPM is reduced, which may explain why the out-of-plane loading increases with a reduction in RPM.

Contrary to the in-plane loading noise increase with RPM reduction, the out-of-plane increase is significant as loading noise is dominant over out-of-plane thickness noise, especially at an elevation angle of -75 deg., where these highly impulsive signals are. This fact should be kept in mind when slowing the rotor RPM of a lift-offset coaxial helicopter to reduce the in-plane thickness noise as decreasing one noise source for certain observer locations, by changing the RPM, appears to increase the other noise source at different observer locations.

Peak OASPL vs. RPM & M_{AT}

As a summary of this coaxial acoustic RPM reduction study, full sphere Overall Sound Pressure Level (OASPL) cases, with an observer sphere radius of 10 rotor radii from the hub, all around the helicopter, were run for 7 different RPMs, varying from the maximum of 345 RPM to 57% of the maximum, or 196 RPM, for a forward flight speed of 250 kts. From these spheres, the peak OASPL was extracted for each RPM case and a plot of the peak OASPL vs. rotor RPM on the bottom x-axis and M_{AT} on the top x-axis is shown in Fig. 28. As it can be seen, the RPM and corresponding M_{AT}, impact the coaxial helicopter noise greatly. For lower RPMs, the noise increase almost linearly with RPM (on a log scale) and at higher RPMs this trend becomes superlinear. This plot serves to further emphasize the overall acoustic advantage of slowing the rotor RPM of a compound coaxial helicopter in high-speed forward flight.

Furthermore, in conjunction with Ref. 3, which showed that a 27% reduction in main rotor RPM, at a forward flight speed of 250 kts, reduced the total power of the XH-59 configuration by 17%, the same RPM reduction decreases the peak OASPL by almost 30 dB! This corresponds to a 97% reduction in acoustic pressure, even without the inclusion of HSI noise! Thus, it is clear that reducing the RPM of a lift-offset coaxial helicopter in high-speed forward flight can lead to dramatic performance improvement and noise reduction.

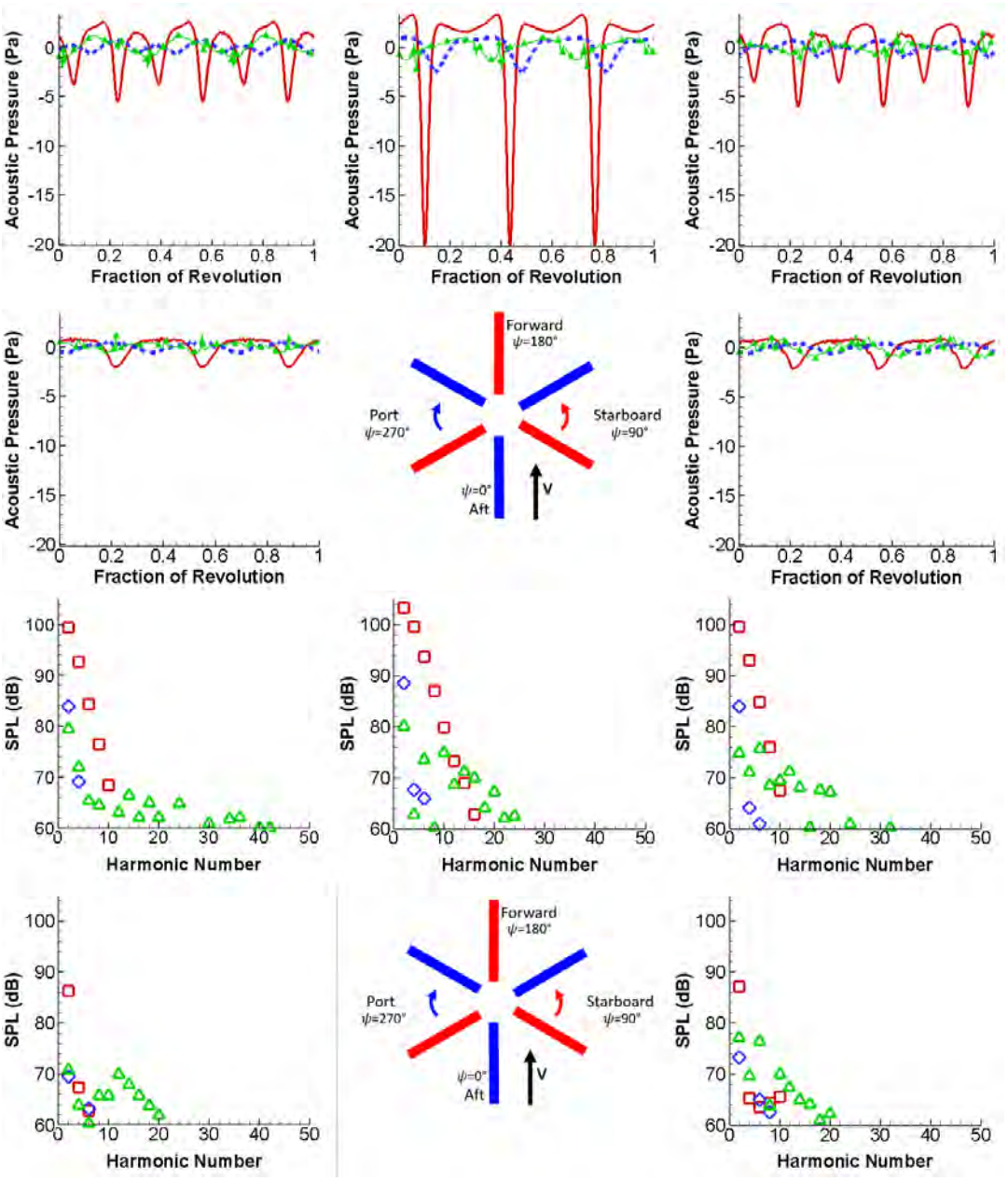

Figure 17. Comparison of total noise at in-plane observers with varying RPM
(□ 276, ◇ 207, △ 179) (M_{AT}: 0.84, 0.72, 0.67).

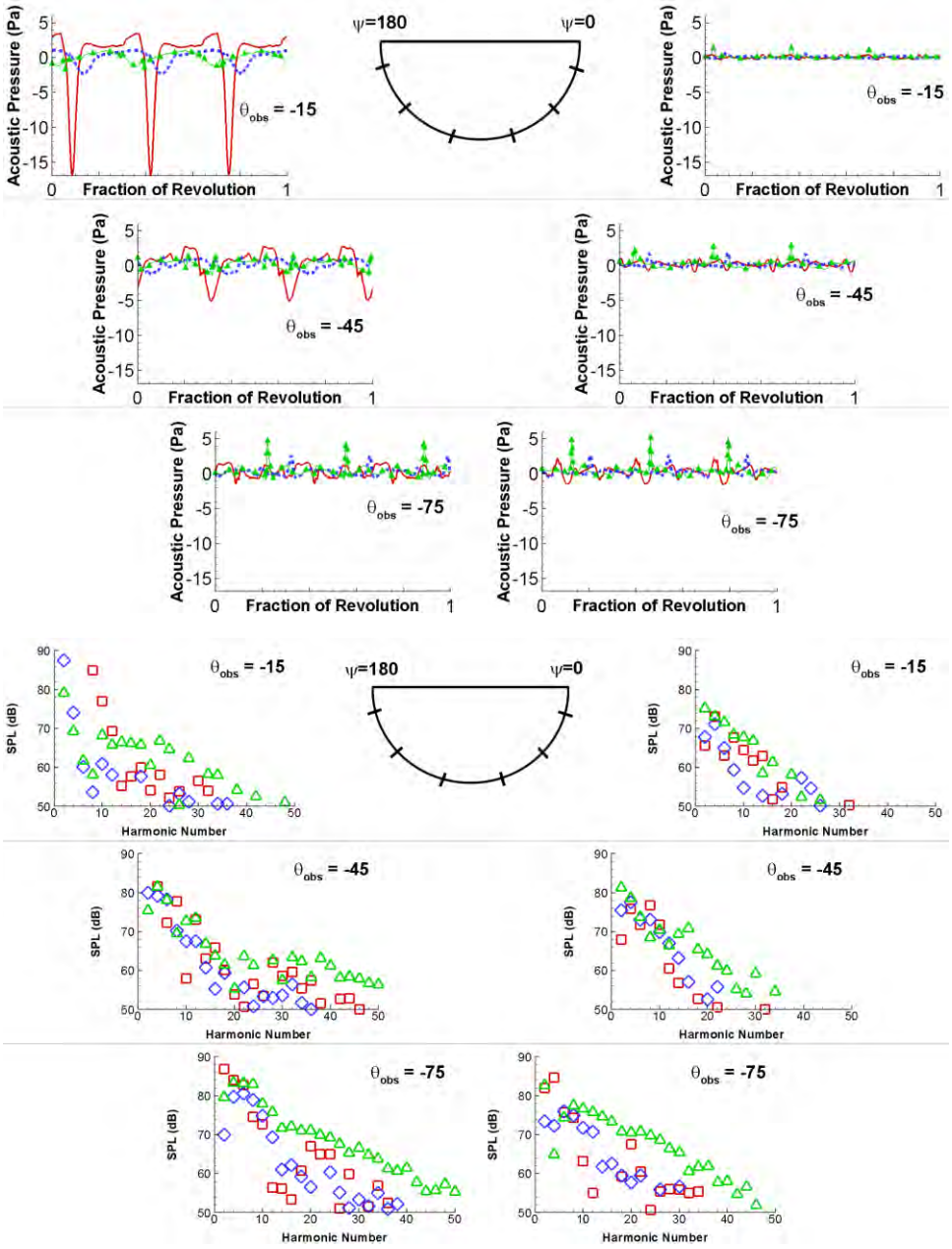

Figure 18. Comparison of total noise at out-of-plane ψ = 0 and 180 deg. observers with varying RPM (□ 276, ◇ 207, △ 179) (M_{AT}: 0.84, 0.72, 0.67).

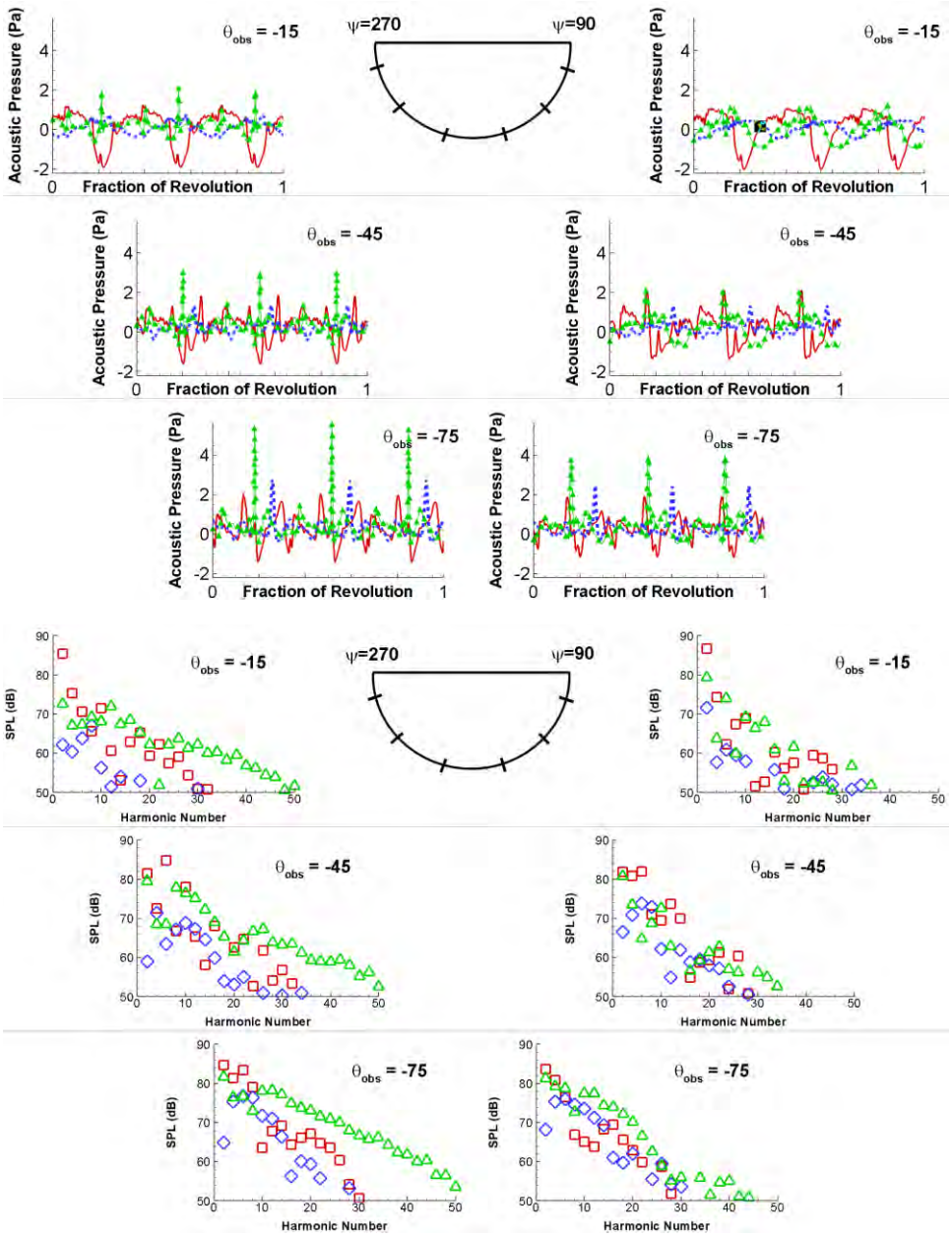

Figure 19. Comparison of total noise at out-of-plane ψ = 90 and 270 deg. observers with varying RPM (□ 276, ◇ 207, △ 179) (M_{AT}: 0.84, 0.72, 0.67).

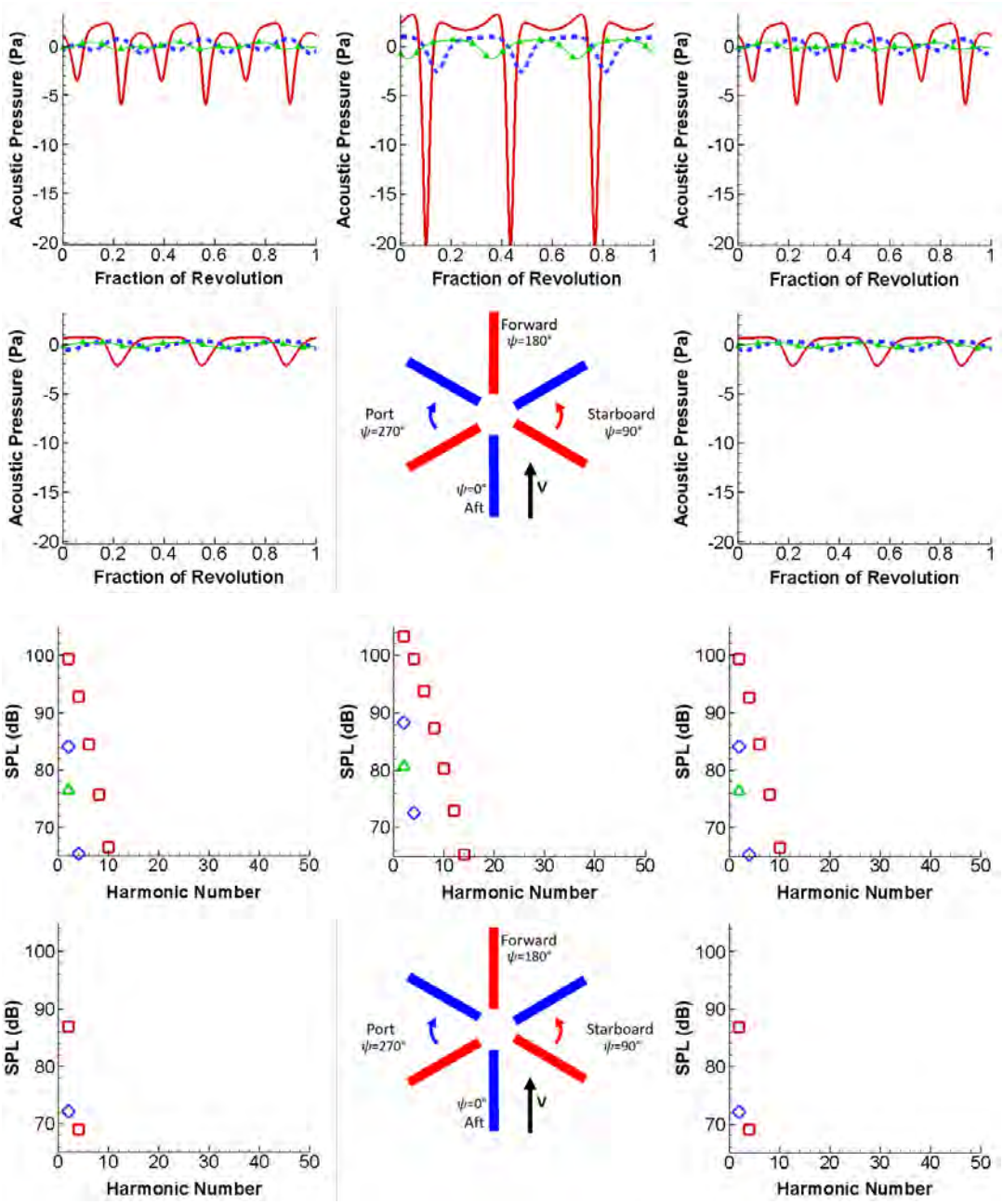

Figure 20. Comparison of thickness noise at in-plane observers with varying RPM
(□ 276, ◇ 207, △ 179) (M_{AT}: 0.84, 0.72, 0.67).

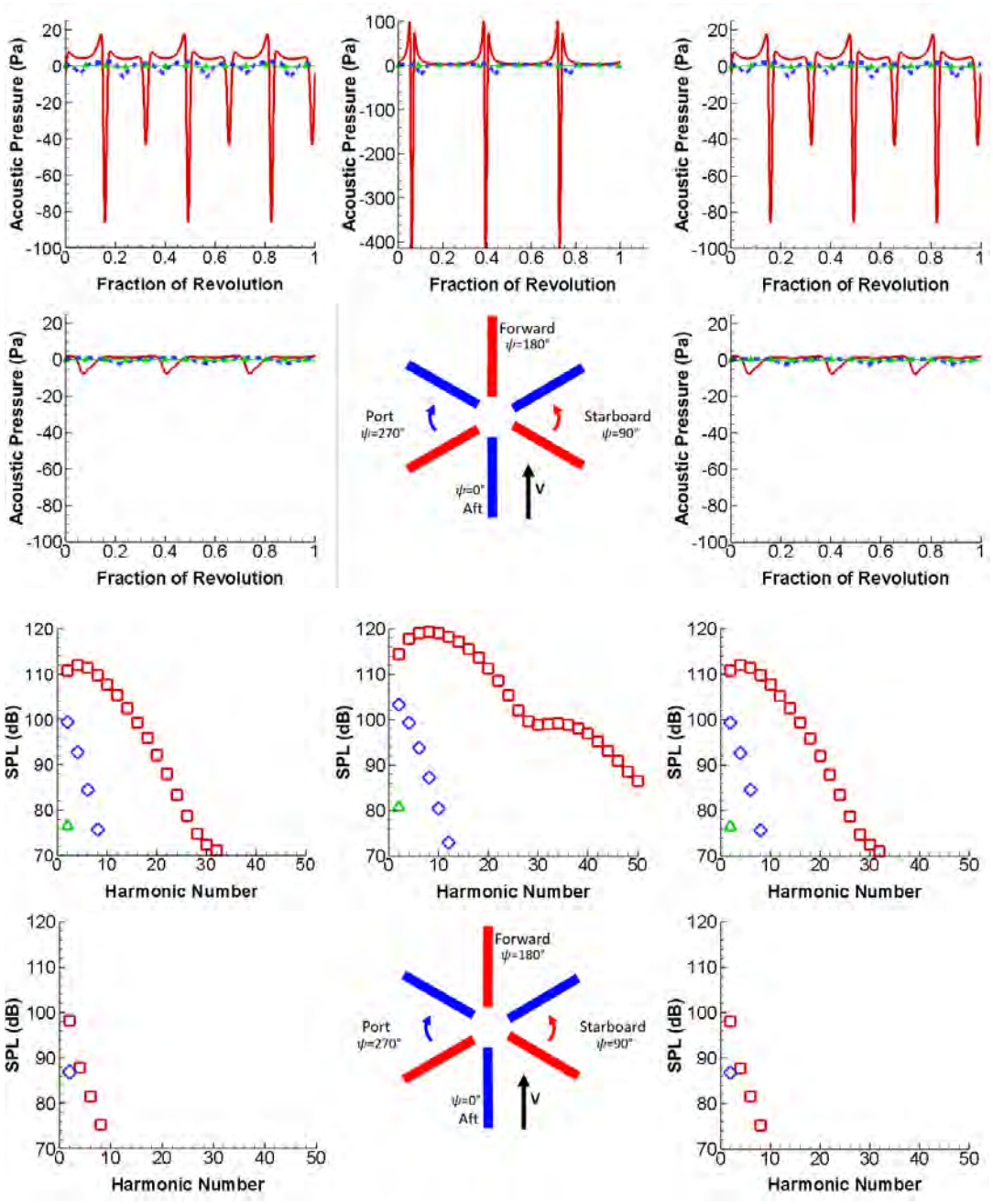

Figure 21. Additional comparison of thickness noise at in-plane observers with varying RPM (—□— 276, ·····◇····· 207, —△— 179) (M_{AT}: 0.84, 0.72, 0.67). Note different scale for top center plot.

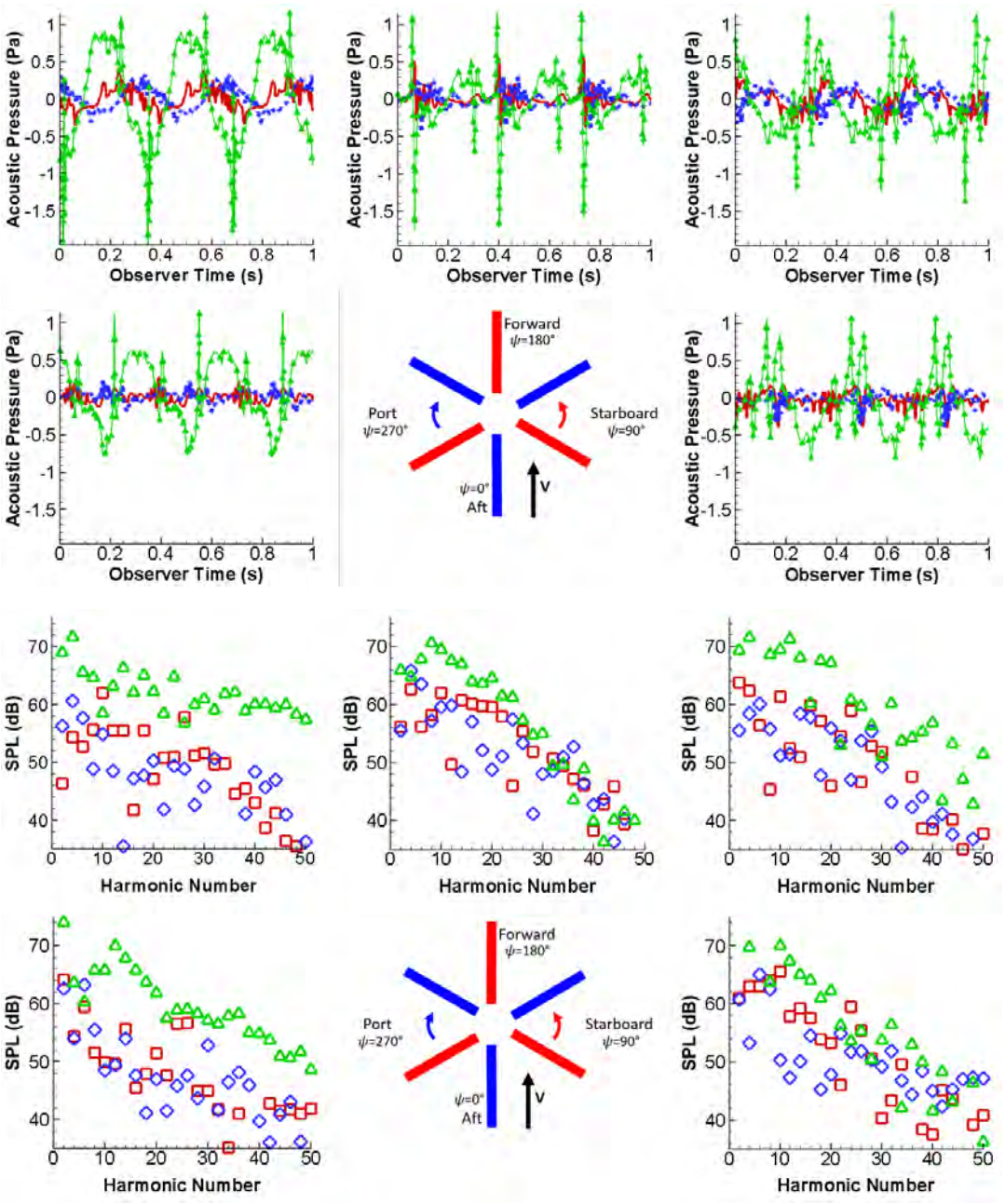

Figure 22. Comparison of loading noise at in-plane observers with varying RPM (——— □ 276, ····· ◇ 207, ——▲—— △ 179) (M_{AT}: 0.84, 0.72, 0.67).

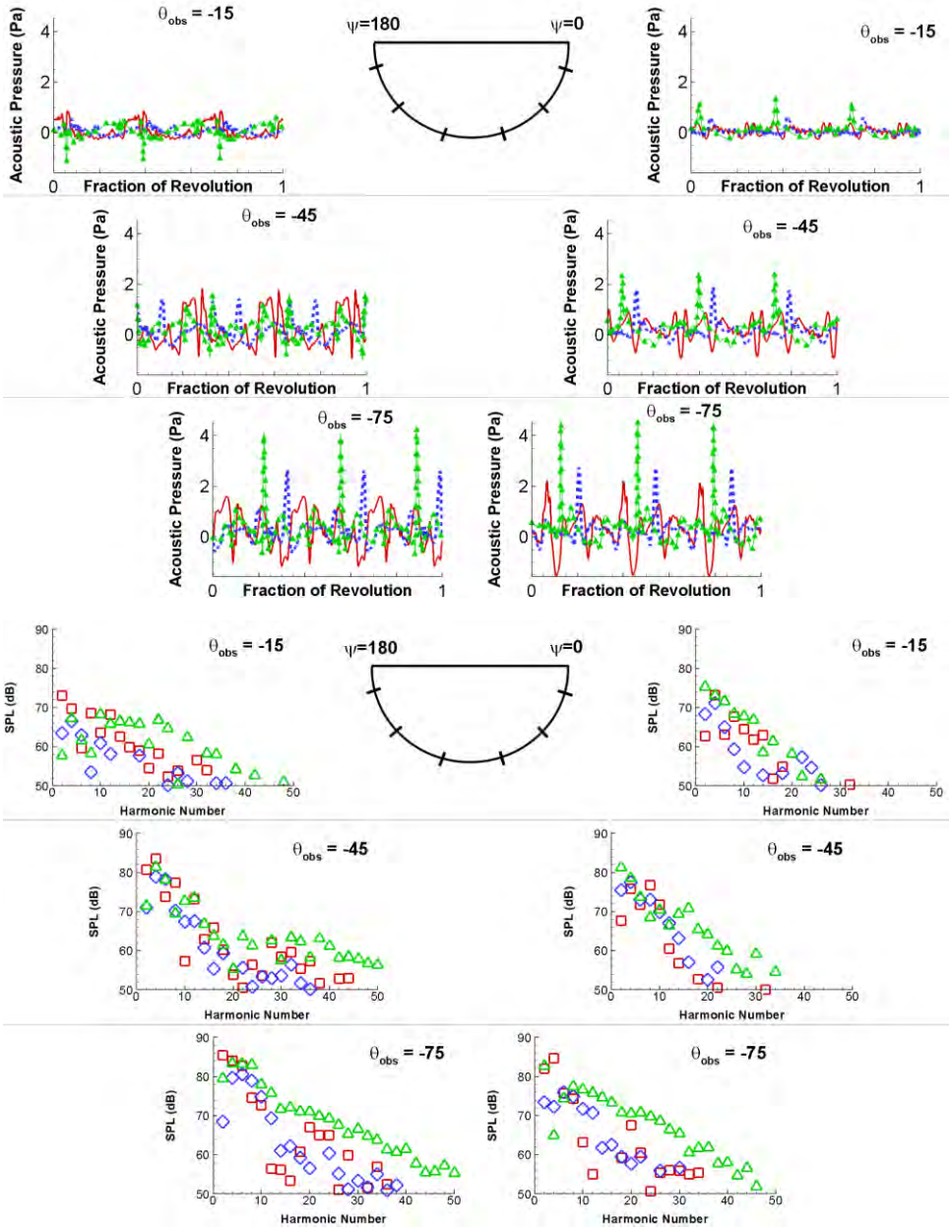

Figure 23. Comparison of loading noise at out-of-plane ψ = 0 and 180 deg. observers with varying RPM (□ 276, ◇ 207, △ 179) (M_{AT}: 0.84, 0.72, 0.67).

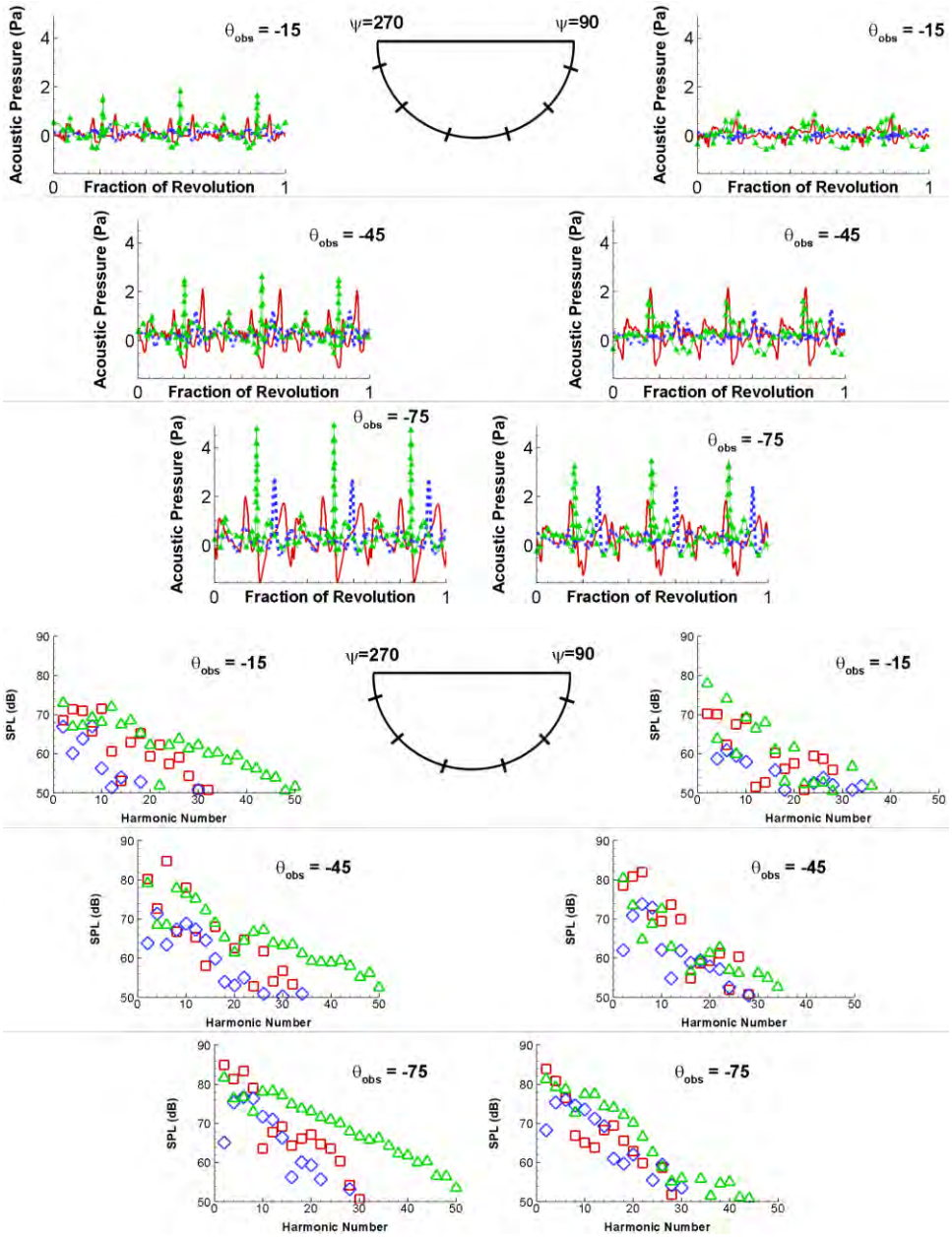

Figure 24. Comparison of loading noise at out-of-plane ψ = 90 and 270 deg. observers with varying RPM (□ 276, ◇ 207, △ 179) (M_{AT}: 0.84, 0.72, 0.67).

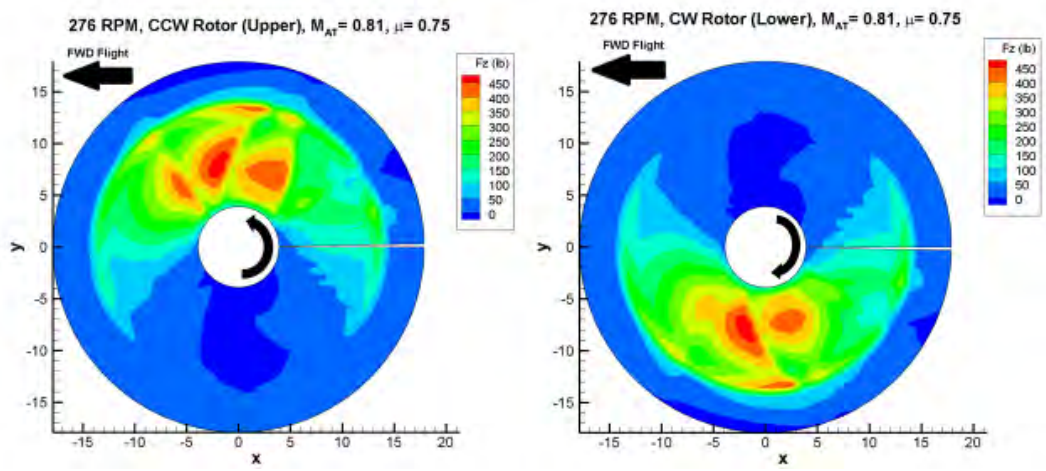

Figure 25. Lift distribution on rotor disk plots for both the CCW, upper (left), and the CW, lower (right), rotors at 276 RPM.

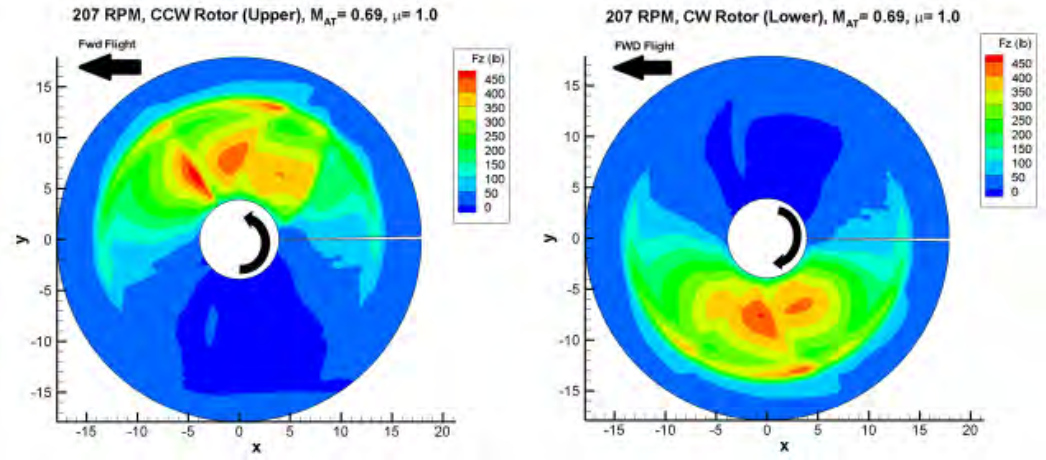

Figure 26. Lift distribution on rotor disk plots for both the CCW, upper (left), and the CW, lower (right), rotors at 207 RPM.

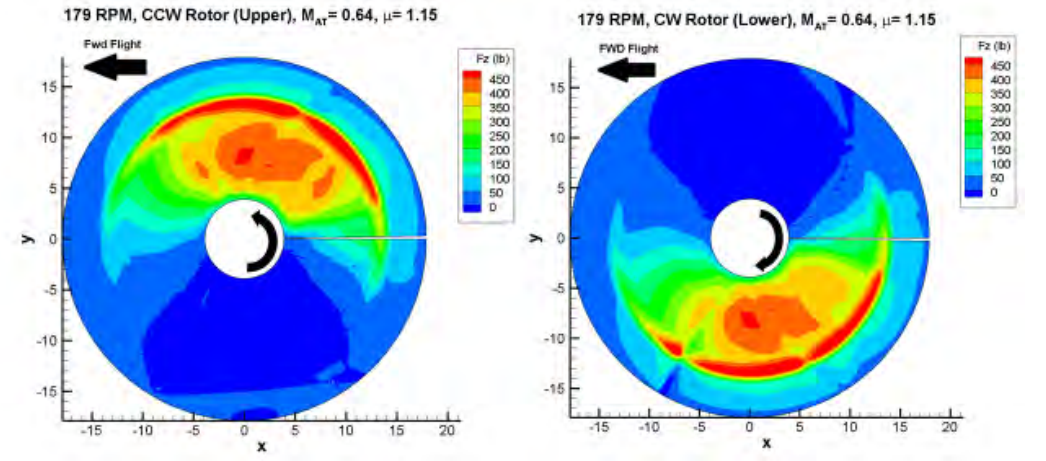

Figure 27. Lift distribution on rotor disk plots for both the CCW, upper (left), and the CW, lower (right), rotors at 179 RPM.

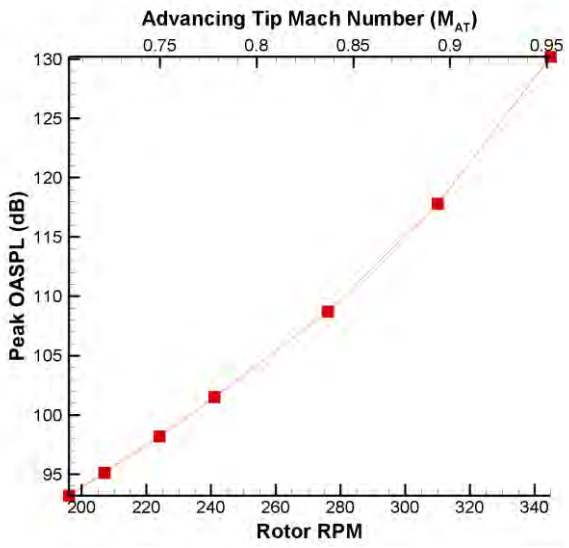

Figure 28. Peak OASPL vs. rotor RPM/M_{AT} for a full sphere of observers 10 rotor radii from the rotor hub of a coaxial rotor.

DUAL-SWEPT TIP BLADES

Both the blade crossover locations and the rotor RPM affected the acoustics of the coaxial helicopter in high-speed forward flight. Another design parameter to consider is the geometry of the blades. There are two motivations to study a planform with significant forward and rearward sweep. First, planform changes, such as double sweep (forward then rearward sweep – i.e., like the Blue Edge rotor blades, Refs. 12-14) have been shown to reduce BVI noise by changing the geometry of the interaction of the blade and the tip vortex. Such a geometry change might also alleviate any blade crossing event in the lift-offset coaxial rotor. The second motivation is that changes in geometry will also lead to changes in the constructive/destructive acoustic interference of the blades at various observer locations. Moreover, on a high-speed rotorcraft configuration, like the XH-59, the swept tips could be essential to enabling high forward speeds by delaying potential shocks on the advancing blades.

Configurations

In order to achieve this desired result, multiple blade designs and configurations were considered but only the three most interesting and most effective designs considered thus far are discussed in this section and shown in Figs. 29, 30 and 31. In Fig. 29, the originally conceived dual swept tip blade design and coaxial configuration is displayed. The first dual-swept tip blade design has forward sweep inboard and reward sweep outboard. Upon acoustically investigating this unique blade design further, a new configuration, shown in Fig. 30, was proposed, which features "anti-symmetric" dual-swept tip blades on the lower, CW rotor. This anti-symmetric configuration has rearward sweep inboard and forward sweep outboard, such that when the blade from the two rotors cross, they have they overlap everywhere, as can be seen in Fig. 30. Finally, as an extension of the "anti-symmetric" blade configuration, the same design as in Fig. 30 is considered except with the blades crossing at ψ = 30 deg. and every 60 deg. after that around the azimuth.

With the goal in mind of exploring these blade designs and reducing the relatively large thickness acoustic signal at in-plane observers, especially at the forward ψ = 180 deg. observer, only the in-plane thickness noise was considered in this study and for brevity, only the results for the ψ = 180 deg. observer are presented in the next section. Each case of this study was run for a forward flight speed of 250kts, at a rotor RPM of 332, resulting in M_{AT}= 0.93, with an observer at a distance of 5 rotor radii from the rotor's hub, half the distance of the cases previously shown.

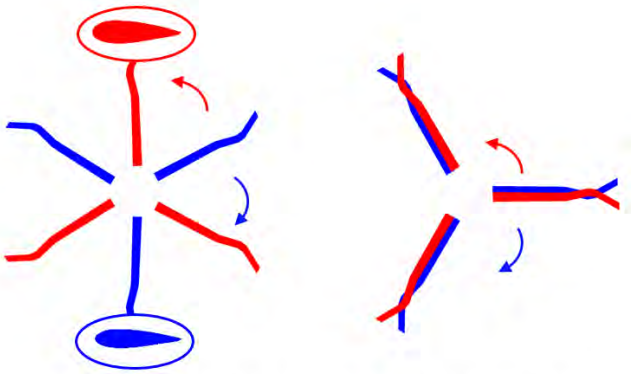

Figure 29. Original dual swept tip blade configuration.

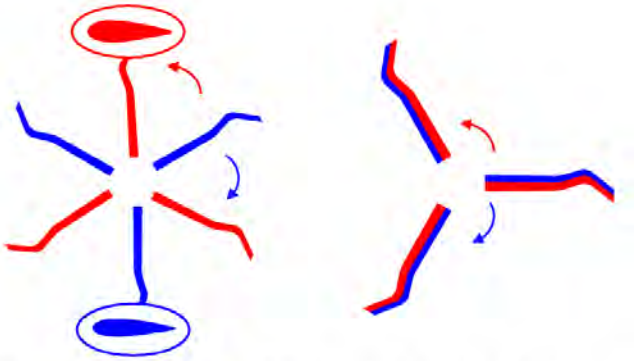

Figure 30. "Anti-Symmetric" dual swept tip blade configuration.

Thickness

The thickness noise results for each of the three configurations described in Figs. 29 and 30, as well as the original XH-59 blade design, are plotted on the same graph and shown in Fig. 31. As illustrated by this plot, each successive design consideration reduced the thickness noise at this target observer, with the smallest signal coming from the "anti-symmetric," ψ = 30 deg. azimuth crossover design. From the previous blade crossover study, it is understood that changing the blade phasing alters the constructive interference of the in-plane thickness noise and this new "anti-symmetric" blade configuration has a similar effect.

As mentioned before, this "anti-symmetric" blade design features advancing blades with outboard sections of both advancing blades all at different distances relative to the forward observer at a given time. Acoustically, this design both widens the acoustic signal as well as weakens it because the individual signals from the upper and lower rotor blades no longer arrive to the observer at the same time. Thus, the constructive interference of these two independent signals is not as strong and a widened summation pulse results. Compounding the "anti-symmetric" blade design with a different blade crossover position draws benefits from both configurations, resulting in the weakest acoustic signal of the considered designs. It should be noted that HSI noise is again not accounted for in these calculations and would have a significant impact; but, sweep near the tip should delay the formation and weaken shocks (and hence reduce the impact of HSI noise to some extent). Nonetheless, these cases are only representative designs that should be further explored with HSI noise included.

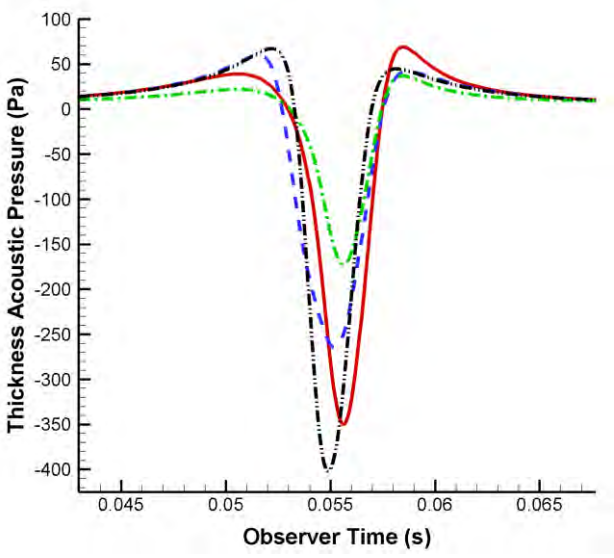

Figure 31. Comparison of thickness noise at the forward, ψ = 180 deg. observer for the three dual swept tip blade designs and the XH-59 blades.

(Original Dual Swept Tip, Anti-Symmetric, Anti-Symmetric with ψ = 30 deg. blade crossover, XH-59).

CONCLUSIONS

Acoustic predictions of a model XH-59 coaxial helicopter for a wide variety of cases and observer locations have been performed.

The acoustic field due to this coaxial rotor design in forward flight is characterized by large thickness acoustic pulses directly forward of the rotor, constructive interference of acoustic signals from the upper and lower rotors for observers at ψ = 0, 90, 180 and 270 deg. and impulsive pressure jumps in the loading noise, specifically below the rotor plane, likely caused by BVI, rotor-rotor interactions or rotor-wake interactions. Each of these characteristics give rise to acoustic concerns, especially at high speeds. However, specific design features and/or trim settings inherent to a compound coaxial configuration enable the effects of these characteristics to be mitigated.

Most notably, decreasing the rotor's RPM while maintaining flight speed provides the greatest benefit by reducing the large in-plane thickness acoustic pulses ahead of the rotor, reducing the overall acoustic signal and producing a performance improvement as well, reducing the total power required. This variable rotor RPM feature is highly valuable and should be exploited when possible.

This paper is a "first look" at the noise generated by lift-offset coaxial helicopters. There are several areas of acoustic "concern" when considering a lift-offset coaxial helicopter, but there are also design changes and operation parameters that can be used to mitigate the noise problem. The findings of this paper suggest that further and more comprehensive studies of lift-offset coaxial rotor noise would be beneficial.

A first step in continuing this area of research would be to run full, high fidelity CFD for these high speed cases, extracting the surface pressures on each blade and using those as loading input for PSU-WOPWOP to more accurately predict loading noise. Further, analyzing the blade loadings around the azimuth to identify specific interactions and when each occurs would also be useful.

With this expanded knowledge, new noise reduction designs and techniques should be explored and those presented in this study should be reevaluated with the new solutions. As compound lift-offset coaxial helicopters become more widely used in both civilian and military applications, noise will become a very important issue that needs to be understood and accurately predicted. This study aimed to serve as an introduction to coaxial helicopter noise with the hope of continued research spawning from it.

ACKNOWLEDGMENTS

This research is partially funded by the Government under Agreement No. W911W6-11-2-0011. The U.S. Government is authorized to reproduce and distribute reprints notwithstanding any copyright notation thereon.

The views and conclusions contained in this document are those of the authors and should not be interpreted as representing the official policies, either expressed or implied, of the U.S. Government.

REFERENCES

[1]Cheney, Jr., M.C., "The ABC Helicopter," AIAA/AHS VTOL Research Design, and Operations Meeting, AIAA Paper 69-127, Georgia Institute of Technology, Atlanta, GA, February 17-12, 1969.

[2]Ruddell, A. J., "XH-59A ABC Technology Demonstrator Altitude Expansion and Operational Tests," Technical Report USAAVRADCOM-TR-81-D-35, U. S. Army Research and Technology Laboratories (AVRADCOM), December 1981.

[3]Johnson, W., "Influence of Lift Offset on Rotorcraft Performance," NASA TP-2009-215404, November 2009.

[4]Mosher, M., and Peterson, R.L., "Acoustic Measurements of a Full Scale Coaxial Helicopter," AIAA 8th Aeroacoustics Conference, AIAA Paper 83-0722, Atlanta, GA, April 11-13, 1983.

[5]Jacobellis, G., Gandhi, F., and Floros, M., "A Physics-Based Approach to Trim Optimization of Coaxial Helicopters in High-Speed Flight," Paper AHS2015-000044, 71st Annual Forum of the American Helicopter Society, Virginia Beach, VA, May 2015.

[6]Saberi, H., Khoshlahjeh, M., Ormiston, R., and Rutkowski, M., "Overview of RCAS and Application to Advanced Rotorcraft Problems," AHS Fourth Decennial Specialists Conference on Aeromechanics, San Francisco, CA, January 2004.

[7]Ffowcs Williams, J. E. and Hawkings, D. L., "Sound Generated by Turbulence and Surfaces in Arbitrary Motion," *Philosophical Transactions of the Royal Society,* Vol. 264, No. 1151, 1969, pp. 321-342.

[8]Brentner, K. S., and Farassat, F., "Modeling Aerodynamically Generated Sound of Helicopter Rotors," *Progress in Aerospace Sciences*, Vol. 39, (2-3), Feb-April 2003, pp. 83-120.

[9]Brès, G. A., Brentner, K. S., Perez, G., and Jones, H. E., "Maneuvering rotorcraft noise prediction," *Journal of Sound and Vibration*, 275(3-5):719-738, August 2004.

[10]Brès, G. A., "Modeling the noise of arbitrary maneuvering rotorcraft: Analysis and implementation of the PSU-WOPWOP noise prediction code," M.S. thesis, Department of Aerospace Engineering, The Pennsylvania State University, June 2002.

[11]Perez, G., "Investigation of the influence of maneuver on rotorcraft noise," M.S. thesis, Department of Aerospace Engineering, The Pennsylvania State University, June, 2002.

. [12]Rauch, P., Gervais, M., Cranga, P., Baud, A., Hirsch, J-F., Walter, A., and Beaumier, P., "Blue Edge: The Design, Development and Testing of a New Blade Concept," Paper AHS2011-000043, 67th Annual Forum of the American Helicopter Society, Virginia Beach, VA, May 2011.

[13]Paur, J. Eurocopter Moves One Step Closer To 'Whisper Mode'. 2010 Feb 25, 2010 [accessed 3/4/2016]; Available from: http://www.wired.com/2010/02/eurocopter-moves-one-step-closer-to-whisper-mode/

[14]Nelms, D. (2015). "New Eco-Friendly Bluecopter Unveiled," *Vertiflite* 61(5): pp. 26-28.